

Spreading Depression Requires Microglia and is Decreased by Their M2a Polarization from Environmental Enrichment

Kae M. Pusic,¹ Aya D. Pusic,^{1,2} Jordan Kemme,¹ and Richard P. Kraig^{1,2}

Microglia play an important role in fine-tuning neuronal activity. In part, this involves their production of tumor necrosis factor- α (TNF α), which increases neuronal excitability. Excessive synaptic activity is necessary to initiate spreading depression (SD). Increased microglial production of proinflammatory cytokines promotes initiation of SD, which, when recurrent, may play a role in conversion of episodic to high frequency and chronic migraine. Previous work shows that this potentiation of SD occurs through increased microglial production of TNF α and reactive oxygen species, both of which are associated with an M1-skewed microglial population. Hence, we explored the role of microglia and their M1 polarization in SD initiation. Selective ablation of microglia from rat hippocampal slice cultures confirmed that microglia are essential for initiation of SD. Application of minocycline to dampen M1 signaling led to increased SD threshold. In addition, we found that SD threshold was increased in rats exposed to environmental enrichment. These rats had increased neocortical levels of interleukin-11 (IL-11), which decreases TNF α signaling and polarized microglia to an M2a-dominant phenotype. M2a microglia reduce proinflammatory signaling and increase production of anti-inflammatory cytokines, and therefore may protect against SD. Nasal administration of IL-11 to mimic effects of environmental enrichment likewise increased M2a polarization and increased SD threshold, an effect also seen *in vitro*. Similarly, application of conditioned medium from M2a polarized primary microglia to slice cultures also increased SD threshold. Thus, microglia and their polarization state play an essential role in SD initiation, and perhaps by extension migraine with aura and migraine.

GLIA 2014;00:000–000

Key words: migraine, hippocampal slice culture, interleukin-11, environmental enrichment, microglial polarization

Introduction

Migraine is a neurological disorder characterized by episodic severe and painful headaches lasting between 4 and 72 h. These low-frequency, episodic events may evolve into higher-frequency and eventually chronic migraine. This transformation may involve increased excitability and related increases in inflammation and production of reactive oxygen species (ROS) (Grinberg et al., 2012, 2013; Viggiano et al., 2011).

Spreading depression (SD), the most likely cause of migraine aura and perhaps migraine, is a benign perturbation of brain, consisting of increased synaptic activity followed by a period of electrical silence (Bureš et al., 1974; Pietrobon and Moskowitz, 2013; Somjen, 2001). Following an episode of SD, neuronal excitability is temporarily elevated (Grinberg et al., 2011; Kruger et al., 1996). Frequent occurrences of SD

without sufficient time to recover may be responsible for the transition from episodic migraine to high-frequency and chronic migraine (Kraig et al., 2010). Few therapeutic options exist to prevent migraine or mitigate the transformation of episodic to high-frequency and chronic migraine. However, environmental enrichment (EE; volitionally increased physical, social, and intellectual activity) has been clinically shown to reduce migraine frequency (Darabaneanu et al., 2011) and SD propagation velocity (Guedes et al., 1996).

EE occurs with physiologically increased synaptic activity that is reflective of learning, and low-level peripheral inflammation produced by increased physical activity (Radak et al., 2008; van Praag et al., 2000). Both these events produce a phasic increase in ROS, a low-level stressor that, given sufficient time to recover, induces an adaptive response (Fuente et al., 2011; Kraig et al., 2010; Sasaki et al., 2013).

View this article online at wileyonlinelibrary.com. DOI: 10.1002/glia.22672

Published online Month 00, 2014 in Wiley Online Library (wileyonlinelibrary.com). Received Oct 30, 2013, Accepted for publication Mar 27, 2014.

Address correspondence to Richard P. Kraig, Department of Neurology, The University of Chicago, Chicago, IL 60637, USA.
E-mail: rkraig@neurology.bsd.uchicago.edu

From the ¹Department of Neurology, The University of Chicago, Chicago, Illinois; ²Committee on Neurobiology, The University of Chicago, Chicago, Illinois.

Adaptive stress responses can include increased production of antioxidants and increased anti-inflammatory signaling that may help protect the brain (Herring et al., 2010; Williamson et al., 2012). Here, we showed that EE-mediated mitigation of SD may involve increased production of anti-inflammatory cytokines, such as interleukin-11 (IL-11).

IL-11 is a pleiotropic cytokine that plays a key role in anti-inflammatory responses, and significantly reduces tumor necrosis factor- α (TNF α ; Trepicchio et al., 1996), including that produced following SD (Hulse et al., 2008). TNF α enhances synaptic efficacy by increasing membrane expression of excitatory α -amino-3-hydroxy-5-methyl-4-isoxazolepropionic acid receptors and decreasing membrane expression of inhibitory γ -aminobutyric acid-A receptors (Stellwagen et al., 2005). Increased neuronal excitability in turn leads to increased ROS production, both of which promote subsequent occurrence of SD (Grinberg et al., 2012, 2013). Though both microglia and astrocytes are capable of TNF α production, we believe that microglial activation is necessary for firing of SD.

Like macrophages, microglia can be polarized to distinct phenotypic types that range from a classically activated state to an alternatively activated state (Kigerl et al., 2009; Ransohoff and Perry, 2009). Current understanding of microglial polarization designates four classes of activation. M1 polarization stimulates production of pro-inflammatory cytokines (e.g., TNF α) and increased generation of reactive oxygen and nitrogen species [i.e., through increased inducible nitric oxide synthase (iNOS)] (Durafort et al., 2012; Liao et al., 2012). Conversely, M2a polarized microglia are characterized by increased production of anti-inflammatory cytokines (e.g., TGF β and IL-10) and neurotrophic factors, and are thought to promote repair and regeneration (Ajmone-Cat et al., 2013; Maiorino et al., 2013). Though additional activation states have been described, including an immunosuppressive phenotype (M2b), and an acquired-deactivation state (M2c) (Chhor et al., 2013), we focus here on M1 *versus* M2a activation states.

In this study, we explored the role of microglia and their polarization in the generation of SD. We found that depletion of microglia in slice cultures lead to an inability to evoke SD whereas replacing microglia in depleted cultures restored susceptibility to SD, suggesting an essential role for these cells. Furthermore, microglial polarization state dramatically impacted SD threshold—both *in vitro* and *in vivo*. Importantly, we found that exposure to EE significantly increased SD threshold in whole animals. This effect could be mimicked through nasal administration of IL-11, which significantly increased both neocortical SD threshold and microglial polarization toward an M2a phenotype. Thus, microglia play an essential role in SD initiation, and manipulation of microglial polarization may be an important focus

for development of migraine therapeutics. This work has appeared in preliminary form (Pusic et al., 2013).

Materials and Methods

Animal Use

All procedures involving animals were approved by the Institutional Animal Care and Use Committee at the University of Chicago, and were conducted in accordance with the guidelines published in the Guide for the Care and Use of Laboratory Animals (2011). Wistar rats were obtained from Charles River Laboratories.

Environmental Enrichment

Twelve male Wistar rats were group housed in a two-layered, 58 cm wide, 88 cm long, and 65 cm high in-house fabricated Marlau-style cage for EE (Fares et al., 2013; Obiang et al., 2011). The bottom layer of the cage consisted of a running wheel for exercise, a resting area, and *ad libitum* access to food and water. The top layer of the cage contained a maze which was changed three times a week; six variations of this maze were utilized. Rats climbed from the bottom to the top layer via ramps, progressed through the maze, and descended down another set of ramps to access food and through one-way doors to return back to the exercise and socialization area. Sufficient space was provided to prevent the emergence of dominant male behavior (Marashi et al., 2003). EE rats were housed in this Marlau-style cage for 35 days, whereas 12 aged-matched nonenriched (NE) rats were single-housed under standard conditions.

At the conclusion of EE/NE exposure, animals were anesthetized with progressive exposure to 100% carbon dioxide (i.e., at a rate of 10–30% of the euthanasia chamber volume/minute). Carbon dioxide exposure was continued for a minute after respiratory arrest before animals were decapitated. Brains were removed, frozen in isopentane at -30°C , which was then lowered to -75°C , and stored at -80°C until further processing for protein extraction, RNA isolation, or staining. Additional EE/NE groups were processed for SD as described below.

Slice Culture Preparation

Brain slice cultures are well-accepted models of their *in vivo* counterpart. However, some have expressed difficulty in eliciting SD in hippocampal slice cultures. Accordingly, we emphasize the aspects of our procedures that produce a robust *in vitro* model of SD that closely parallels that found *in vivo*. These features include specific aspects of prenatal care, culture preparation and growth, as well as experimental use.

Untimed pregnant Wistar female rats were single-housed with Enviro-dri[®] paper bedding (Shepherd) and Nestlets (Ancare). This maternal nesting enrichment increased slice culture vitality at 21 days *in vitro* from 80–85% ($n \geq 104$ litters) to 95–100% ($n \geq 156$ litters), and most often 100% (Pusic and Kraig, 2014; Pusic et al., 2014). Pups (culled to 10 at birth) were used for hippocampal slice cultures.

Preparation and growth of hippocampal slice cultures generally followed protocols previously described (Kunkler and Kraig 1997;

Mitchell et al., 2010) with important additional steps. Rat pups (P9-P10) were progressively anesthetized with 100% carbon dioxide (as described above for adult males), decapitated, and their brains removed under sterile conditions. Hippocampi were sliced into 350 μm sections and placed onto Millicell (Millipore) inserts in six-well plates containing a horse serum-based medium (Kunkler and Kraig, 1997). Cultures were grown in horse serum containing medium, and transferred to a serum-free medium after 18 days *in vitro* to remove potential confounding impact of horse serum on detection of immune signaling (Hulse et al., 2008; Pusic and Kraig, 2014; Pusic et al., 2014). Cultures were screened for viability at 21 days *in vitro* with Sytox (Invitrogen), a fluorescent stain for cell death (Hulse et al., 2008). Cultures that lacked evidence of stratum pyramidale neuronal death were considered viable, and thus suitable for subsequent experimental use.

We used hippocampal slice cultures maintained *in vitro* for 21 to 35 days to model SD *in vivo*, since culture in this window of time closely parallel the *in vivo* counterpart (for review see Kunkler et al., 2005 and Pusic et al., 2014). Specifically, the neurovascular unit (Kovacs et al., 2011), multisynaptic electrical activity (Kunkler and Kraig, 1998), pyramidal neuron vitality (Hulse et al., 2008), responsive astrocytes and microglia (Grinberg et al., 2011; Ransohoff and Perry, 2009) and cytokine signaling (Kunkler et al., 2004) resemble that seen *in vivo*. Use of this culture preparation has the additional benefit of allowing microenvironmental conditions to be accurately controlled.

Additionally, modulation of brain tissue extracellular space can influence brain excitability, including that seen with SD (Martins-Ferreira et al., 2000). To our knowledge, the extracellular space has not been studied in brain slice cultures. However, the acute brain slice preparation may provide insights. Submerged acute brain slices show extracellular volume values that are close to those found *in vivo* (Hounsgaard and Nicholson, 1983). Furthermore, interface acute slices show a reduction in extracellular space of about 7% compared with submerged slices (Schuchmann et al., 2002). It seems reasonable to conclude, as a first estimate, that the extracellular space of brain slice cultures as used here (i.e., in an interface configuration) would show a similar reduction in extracellular space that could modestly enhance excitability compared with their *in vivo* counterpart.

Use of an interface configuration is essential for induction of SD in slice cultures (Kunkler and Kraig, 1998) as it is with acute brain slices (Snow et al., 1983). However, several other experimental use parameters are important to ensure robust induction of SD, as opposed to confounding perturbations of spreading depolarizations, seizures, or spreading convulsions (Dreier et al., 2011; Pomper et al., 2006).

It is our experience that induction of SD in hippocampal brain slice cultures maintained in horse serum-based medium is difficult or impossible. This initially led us to expose cultures to a Ringer's solution that was transiently altered to a chloride free Ringer's to induce SD (Kunkler and Kraig, 1998, 2004; Kunkler et al., 2005). Unfortunately, this method of stimulation can sometimes preclude induction of SD due to alternative induction of bursting activity or seizures (Kunkler and Kraig, 1998) like that seen by Pomper and

coworkers when using less mature cultures (Pomper et al., 2006). Such confounds have been resolved by the following additional procedures. First, we have shown that cultures require at least 15 mM glucose for optimal function; our habit is to use 42 mM glucose, as originally described for preparation of brain slice cultures. Second, we do not expose cultures to oxygen levels above that found in room air ($\sim 20\%$), as this tends to provoke seizures, which prevent induction of SD. Third, we do not use penicillin/streptomycin since this antibiotic combination, unlike gentamycin, provokes seizure activity. Fourth, physiological recordings (as well as all manipulations) are completed while cultures are exposed to normal serum-free medium, not Ringer's, since the latter reduces culture vitality over hours. Fifth, our serum-free medium contains glutathione, as well as cysteine, glycine, and glutamate which are essential to maintain cellular glutathione levels. Also, the medium contains ascorbate and tocopherols and the antioxidant enzymes catalase and superoxide dismutase as noted in Grinberg et al., 2013 (Gemini BioProducts Material Data Safety Sheet; Brewer et al., 1993).

The above steps allow us to create physiologically robust and long-lived brain slice cultures with neural cells, cytokine levels, and responses to pathological perturbations (e.g., SD, NMDA injury, multiple sclerosis modeled with lysolecithin) like that seen *in vivo*. As use of serum-free medium is essential for the induction of SD in slice cultures, we specifically provide the formulation here. Serum-free medium, per 100 mL, consists of: Neurobasal medium (97 mL; Invitrogen); Gem21 NeuroPlex supplement, (2.0 mL; Gemini Bio-products); GlutaMax (1 mM; Invitrogen); gentamicin (1 $\mu\text{g}/\text{mL}$; Invitrogen); D-glucose (45%; 680 μL ; Sigma); ascorbic acid (0.5 mM; Sigma); Fungizone, (1 mg/mL; Invitrogen); NaCl (41 mM; Sigma); Mg_2Cl_2 (0.8 mM; Sigma); CaCl_2 (1.6 mM; Sigma). Constituents of Neurobasal are detailed by Brewer et al. (1993) and include an array of amino acids and vitamins as well as traditional salts. Gem21 was used as previously described (Chen et al., 2008), and provided insulin, T3, and the antioxidant agents noted above. (Gemini Bio-Products Material Data Safety Sheet; www.gembio.com).

Isolation of Primary Microglia

Primary microglia were cultured as previously described (Caggiano and Kraig, 1998). Briefly, postnatal Wistar rat pups (P0-P3) were progressively anesthetized with 100% carbon dioxide, washed in ethanol, decapitated, and brains harvested. The meninges were carefully removed, and the cortices dissected out in Hanks' Balanced Salt Solution (Invitrogen) without calcium or magnesium. Tissue was then dissociated by trituration in Hank's Balanced Salt Solution containing 10% trypsin (Gibco) and then incubated for 15 min at 37°C with agitation. Filtered fetal bovine serum (FBS; Gibco) and DNase (Invitrogen) were added to neutralize trypsin, and the solution vortexed and then spun down at 2,000 rpm for 5 min. The resultant pellet was washed twice in culture medium [Dulbecco's Modified Eagle Medium (DMEM; Invitrogen) with 10% FBS], resuspended at $\sim 2 \times 10^7$ cells per 12 mL, and plated in 75 cm^2 flasks (Corning). Medium was changed every 3 to 4 days. At 10 to 14 days postculture, flasks were shaken (150 rpm for 10 min at room temperature) to release the loosely adherent microglial

population from the adherent astrocyte monolayer. Cells were collected, washed, and re-plated on flamed glass coverslips (Corning) at $\sim 1 \times 10^6$ cells, or added to clodronate treated slice cultures for rescue experiments (see below).

Microglia cultures were maintained in DMEM medium supplemented with astrocyte-conditioned medium in a 1:1 ratio, and were ready for use in subsequent experiments 3 days later. Astrocyte conditioned medium was prepared by harvesting culture medium from cultured astrocytes 24 h after feeding with DMEM supplemented with 10% FBS (Sievers et al., 1994). Supplementation with astrocytes conditioned medium improves the growth and longevity of cultures and produces ramified (i.e., quiescent) microglia (Eder et al., 1999; Frei et al., 1986). Iba1 staining was performed to confirm that microglial cultures were >95 to 99% pure (data not shown). Additionally, staining for common polarization markers determined that, at baseline, these microglial cultures do not show a dominant polarization state (data not shown).

Primary microglia cultures were polarized through treatment with either IL-4 (M2; 20 ng/mL; R&D Systems) or lipopolysaccharide (LPS, M1; 1 μ g/mL; Sigma) for subsequent collection of conditioned media (Chhor et al., 2013; Girard et al., 2013; Kigerl et al., 2009). Microglial cultures were additionally treated with IL-11 [100 ng/mL; R&D Systems (Mitchell et al., 2011)] and coverslips fixed for staining.

Use of Clodronate Liposomes

Though all clodronate formulations available (including our own in-house initial fabrications) were made using aseptic techniques, we occasionally found these formulations resulted in infection many days after application to naïve slice cultures. Thus, clodronate liposomes were ultraviolet light sterilized [exposure to 254 nm ultraviolet light for 2 h before use (100 μ W/cm²)]. Ultraviolet light treatment did not adversely affect the ability of clodronate liposomes to deplete microglia.

To deplete the microglia population (Kreutz et al., 2009; Markovic et al., 2005; Vinet et al., 2012), clodronate liposomes (FormuMax or NanoEncapsula) were added to hippocampal slice cultures 18 days *in vitro* at a concentration of 0.5 mg/mL (500 μ g total of encapsulated clodronate; based on manufacturer's information) and incubated at 37°C for 24 h. After 24 h, cultures were gently washed with Neurobasal medium (Invitrogen) and given another dose of 0.5 mg/mL of clodronate liposomes and incubated for an additional 24 h at which point cultures were washed again, placed in new medium, and incubated for 7 days. On day 7, cultures were depleted of microglia and were ready for subsequent experiments.

For rescue experiments, cultured primary microglia ($\sim 5 \times 10^5$ cells in 200 μ L) were added on top of slice cultures. To assess growth and viability, microglia from the same isolation were simultaneously plated on cover-slips at the same density. Two days later, SD threshold was determined in microglia-supplemented, clodronate-treated slice cultures.

Slice Culture Electrophysiology

Hippocampal slice cultures were subjected to experimental treatments before electrophysiological recording. Treatment groups consisted of: 100 ng/mL of IL-11 applied 3 days before recording,

minocycline (10 μ g/mL; Sigma) applied acutely before recording, clodronate liposome treatment (as described above), or treatment with M1/M2a conditioned medium 3 days before recording. Where appropriate, the effect of treatment was assessed at 3 days post application, as this is a commonly used time point for studying delayed neuroprotection (Hulse et al., 2008), which involves *de novo* protein synthesis and requires sufficient time to be maximally evident (Gidday, 2006; Kariko et al., 2004; Stenzel-Poore et al., 2007).

Slice culture electrophysiology was performed as previously described (for detailed protocol see Pusic et al., 2011). Briefly, the hippocampal slice culture insert was placed in a 35-mm culture dish filled with 1.5 mL of serum-free culture medium and secured in place with three small 2 to 4 mm lengths of rubber tubing placed equidistantly around the insert. Another 1 mL of medium was used to saturate a sterile cotton strip that was then placed along the inner wall of the insert to provide necessary humidity. Next, the insert-dish assembly top was covered with polyvinyl chloride wrap (Thermo Fisher Scientific) and placed into a recording chamber (PDMI-2; Harvard) that provide heating to 36°C and 5% carbon dioxide, 95% air. Recording microelectrodes and a specially fabricated bipolar stimulating electrode (Pusic et al., 2011) were positioned into slice cultures using WR 60 manipulators (Narishige).

Interstitial DC recordings were made using an Axoprobe A1 amplifier system coupled to a Digidata 1322A analog-digital conversion board (both from Axon Instruments) run on a PC-based computer system. Bipolar electrical stimuli were provided via a digital Master-8 stimulator (A.M.P. Instruments) coupled to a model BSI-2 isolator (Bak).

For trans-synaptically induced SD, the bipolar stimulating electrode was placed at the dentate gyrus, and recordings made from a microelectrode (filled with 150 mM sodium chloride) placed in the stratum pyramidale of CA3. Before use in SD experiments, slice culture electrophysiological function was assessed by recording CA3 area field potentials. Stimuli (100 μ s pulses, ≤ 0.2 Hz) were applied to the dentate gyrus, and the recording electrode moved along the long axis of the stratum pyramidale of CA3 until the field potential excitatory post-synaptic response was maximal. Slices with greater than 3 mV postsynaptic responses, indicating normal excitability, were used for experiments (Pusic et al., 2011; Grinberg et al., 2012, 2013). To determine SD threshold, stimulation [10 pulses, 10 Hz (100 μ s/pulse)] was applied at half the current required for eliciting maximal field potential, and was then incrementally increased per trial (spaced every 3 min) until SD was induced.

SD was also induced by transient slice exposure to KCl. While recording from the CA3 stratum pyramidale as described above, a small borosilicate glass tube (1.0 mm outside diameter, 0.58 mm inside diameter; Sutter) filled with 1 M KCl-3.5% agar was touched to the dentate gyrus area using a micromanipulator (WR-60, Narishige) for 1 to 2 s to trigger SD. Since the KCl was in a semi-solid form, and the application period was short, we do not believe lingering KCl in the chamber was a confounding factor.

Intranasal Administration of IL-11

Wistar rats were nasally administered one mg of recombinant rat IL-11 (R&D Systems). Rats were placed in a fume hood with a heat

lamp and thermo-regulator to maintain a body temperature of 37°C. Inhalational isoflurane anesthesia was delivered via a nose cone (5% induction and 2–3% maintenance, in oxygen; Baxter). One mg of IL-11 in 50 µL of sodium succinate buffer was administered over a 20-min period at a rate of 5 µL every 2 min to alternating nostrils (Liu et al., 2001). Controls were nasally administered sodium succinate buffer alone.

One day post nasal administration, animals were anesthetized with progressive exposure to 100% carbon dioxide and decapitated. Brains were removed, frozen in isopentane at –30°C, which was then lowered to –75°C, and stored at –80°C until processing for protein extraction, RNA isolation, or staining. Additional groups were processed for SD as described below.

Whole Animal Electrophysiology

Whole animal SD recordings were completed using aseptic techniques (Kraig et al., 1991). Male Wistar (300–400 g) rats were anesthetized with isoflurane in oxygen (5% induction, 3% during surgical procedures, and 2–3% during recordings) via an inhalational mask with outflow gas exhausted via vacuum to prevent room contamination. Arterial oxygen was monitored throughout with an oximeter (Nonin Medical) and ranged from 95 to 100%.

We chose to use isoflurane in accordance with the manufacturer's directions and administered via spontaneous respiration to avoid potential confounds associated with intubation and subsequent animal health. This choice was based on our long-term goal of studying the impact of recurrent SD, which necessarily involves survival surgeries and recurrent anesthesia for electrical recordings. Several points are noteworthy with application of this anesthetic plan. First, in our experience, use of gaseous anesthetics with volitional breathing commonly requires 2 to 3% anesthetic (Kraig et al., 1991). Second, the percentage of inhalational anesthetic administered is influenced by the magnitude of facial mask suction used to prevent gas escaping to the general laboratory environment. Therefore, percentage of inhalational gas cannot be directly compared with that used when animals are under ventilation control via intubation. Third, use of nitrous oxide to reduce the level of isoflurane otherwise necessary will also impact measurements of SD threshold. Nitrous oxide reduces SD frequency, whereas 100% oxygen has no impact (Kudo et al., 2008). Fourth, inhalational isoflurane as used here might have an impact on blood brain barrier opening (Tetrault et al., 2008), and Lapilover et al. (2012) show that peri-infarct blood brain barrier dysfunction facilitates SD. However, if this confound were present in our experiments, it would serve to increase SD susceptibility, which only supports the efficacy of EE or IL-11 for protection against induction of SD. Furthermore, it would be a systematic error since it would equally apply to sham controls and experimental animals.

Once anesthetized (i.e., no withdrawal response to paw pinch), animals were mounted in a standard table-top nose clamp and ear bars and kept warm with an overhead infrared lamp to keep core temperature at 37°C in preparation for cranial surgery. Eyes were coated with Artificial Tears (Akorn) and the head was shaved and cleansed with Betadine (Purdue Products). Next, 0.05 mL Bupivacaine (Hospira) was injected subcutaneously to either side of what

would become a midline scalp incision minutes later. A midline scalp incision was made from just behind the eyes to the lambdoid suture area. The skin was spread laterally and skull scraped free of connective tissue. Skull hemostasis was achieved using Bone Wax (Ethicon). Two 1 to 2 mm craniotomies were made in the left skull under saline cooling and without damaging the underlying dura. The KCl stimulation craniotomy was placed –2.0 mm from Bregma and 1.5 mm to the left of the sagittal suture. The recording craniotomy was placed –6.0 mm from Bregma and 4.5 mm lateral to the sagittal suture.

Anesthetized animals were then quickly transferred from the surgery area to the stereotaxic recording setup where gaseous anesthesia, oxygen monitoring, and warming was continued. The skull was warmed (37°C) directly with sterile saline superfusion. For interstitial DC recordings, a 2 to 4 µm tip microelectrode was positioned 750 µm below the pial surface at the posterior craniotomy with a Canberra micromanipulator (Narishige) and recordings begun using an Axoprobe A1 amplifier system and Digidata 1322A analog-digital conversion board run on a PC-based computer system. For KCl-induced SD threshold measurements, a microelectrode with tip broken to 8 to 12 µm (1.0 mm outside diameter, 0.58 mm inside diameter; Sutter) and filled with 0.5 M KCl was positioned 750 µm below the pial surface at the anterior craniotomy. Micro-injections of KCl were administered via pressure from a Picospritzer-II electronic valve system (General Valve), whose injection periods were registered directly to the permanent digital recording of SD induction. Immediately after SD induction, injection electrodes were raised and moved into a microscope slide with depression wells (Thermo Fisher Scientific) filled with light oil (3-In-ONE). Successful KCl injection stimuli were then delivered into the light oil and the diameter of resultant injection volumes determined using a compound microscope fitted with an optical micrometer within an eye piece.

Measurements of Oxidative Stress

Oxidative stress [(OS), i.e., excess production of oxidants over that of anti-oxidants] was measured using CellROX Deep Red Reagent (Invitrogen), a cell-permeant fluorogenic probe. CellROX was used as previously described (Grinberg et al., 2012, 2013).

While use of CellROX without addition of an exogenous stressor would give a readout of changes in baseline oxidative status under treatment conditions, we were interested in the ability of slice cultures to react to increased oxidative load, such as that produced by SD (Grinberg et al., 2012, 2013). Thus, menadione treatment (8.6 µg/mL; Supelco Analytical) was used to generate reactive oxygen species, and resultant oxidative stress determined (via CellROX fluorescence) as a measure of differential oxidative tolerance of slice cultures subjected to treatment compared with control conditions. However, measurements of baseline oxidative stress and menadione-induced oxidative stress following treatment with M1/M2 conditioned medium produced the same results.

Briefly, IL-11 (100 ng/mL) or M1/M2 conditioned medium was applied to naïve slices for three hours then co-incubated with CellROX and menadione for two hours. CellROX fluorescence intensity was quantified at the CA3 stratum pyramidale via digital imaging strategies as described below.

Following treatment of slice cultures with IL-11 (100 ng/mL), changes in microglial glutathione levels were assessed by co-staining with ThiolTracker (Invitrogen) and isolectin GS-IB₄ AlexaFluor 594 conjugate (1:20; Invitrogen). ThiolTracker is a fluorescent dye that reacts with reduced thiols in intact cells, which predominantly reflect glutathione (Mandavilli and Janes, 2010). Procedures for staining followed manufacturer's protocol, modified for use with hippocampal slice cultures. ThiolTracker was dissolved in dimethyl sulfoxide (2 mM, Sigma) and used at 20 μ M in a thiol-free solution. Culture inserts were rinsed with Gey's balanced salt solution (Sigma) supplemented with 7.25 mL 45% D-glucose (Sigma) to remove extracellular thiols, then incubated in glucose-supplemented Gey's containing ThiolTracker for 30 min under standard conditions. Postincubation, inserts were washed in Gey's, fixed in 10% phosphate buffered formalin at 4°C overnight and stained.

ThiolTracker and CellROX fluorescence intensity was quantified using a self-calibrating sensitive CCD digital imaging system consisting of a QuantEM-512SC camera (Photometrics), electronic shutter (Lambda SC Smart Shutter; Sutter Instruments), and a 100 watt Hg light on a DMIRE2 inverted microscope (Leica) at 20 \times gain. A standardized area of interest at the CA3 stratum pyramidale was used for all quantifications and digital images were thresholded and the average optical intensity registered using MetaMorph software (ver. 7.5.4.0; Molecular Devices).

Although protein carbonylation is ROS-mediated and does not encompass RNS-mediated damage, its measurement is accepted as a reliable indicator for the extent of oxidative damage (Ghezzi and Bonetto, 2003). Protein carbonyl levels were measured utilizing the Protein Carbonyl Content Assay Kit (Abcam) according to manufacturer's protocol. Briefly, protein was extracted from the neocortex of animals nasally administered with IL-11 or sham controls using RIPA buffer as previously described (Cook et al., 2011; Roundtree et al., 2011). Protein homogenate was treated with streptozocin to remove any nucleic acid contaminants. Samples were reacted with 2,4-dinitrophenylhydrazine followed by quantification of the acid hydrazones at 405 nm. BCA assays (ThermoFisher Scientific) were simultaneously run and a standard curve constructed for the calculation of protein carbonyl content based on optical density.

Immunocytochemistry and Microscopy

Hippocampal slice cultures were fixed in 4% paraformaldehyde at 4°C overnight before staining. For whole brain samples, frozen brains were sectioned (40 μ m) using a Leica cryostat (Leica), and fixed in 10% buffered formalin phosphate for 15 min before staining. Primary antibodies used in this study are: monoclonal mouse anti-CNPase IgG (1:1000, Millipore), polyclonal rabbit anti-Iba1 IgG (1:1,000, Wako Pure Chemical Industries), monoclonal mouse anti-GFAP IgG (1:1,000, Santa Cruz Biotechnology), monoclonal mouse anti-NeuN IgG (1:1,000, Millipore), monoclonal mouse anti-Arginase-1 IgG (1:500, BD Biosciences), monoclonal mouse anti-CD32 IgG (1:500, BD Biosciences), and polyclonal rabbit anti-IL-11 IgG (1:10, Santa Cruz Biotechnology). Slices were then incubated with AlexaFluor 488 or AlexaFluor 594 labeled secondary antibody specific to the appropriate animal species (1:1,000, Millipore) and mounted using Prolong Anti-fade with or without DAPI (Invi-

trogen). Fluorescently stained slices were then visualized by either using the Leica TCS SP5 II AOBs laser scanning confocal microscope (Leica) at the Light Microscopy Core Facility at the University of Chicago or a DMIRE2 inverted microscope (Leica). All confocal images were with taken as 11 μ m-thick z-stacks acquired at 63 \times gain.

RT-QPCR

RNA was extracted from slice cultures by TRIzol extraction followed by miRNeasy mini kit (Qiagen) spin column-based purification. Concentrations were measured via RiboGreen (Invitrogen). RNA samples were reverse transcribed in 20 μ L reactions using the iScript cDNA synthesis kit (Bio-Rad) following manufacturer's protocol. Real-time PCR using 1 μ L of cDNA and iQ SYBR Green Supermix (Bio-Rad) were run on the MyiQ Single-Color Real Time Detection System (Bio-Rad). All primers (see Table 1) were used at 10 nM (IDT). Briefly, each sample was normalized to an endogenous control, Rpl13a, and the fold changes for each gene assayed was determined via the delta delta Ct method (Pfaffl, 2001).

Data Handling and Statistics

Data were analyzed using SigmaStat software (v.3.5; Systat Software). All data were subject to normality testing (P value to reject: 0.05), equal variance testing (P value to reject: 0.05), and power ($1 - \beta$: >0.8). Mean control data in each experiment were scaled to 1.00 with all subsequent parameters scaled proportionally to better allow inter-experiment comparisons. Molecular biological data (semiquantitative RT-PCR) analyses and immunohistochemical quantifications included two or more technical replicates per experimental (i.e., biological) measurement. All experimental groups consisted of biological replicates of $n \geq 3$. For semi-quantitative RT-PCR data, fold changes of greater than two were considered significant (Pfaffl, 2001). Pairwise comparisons were made with the Student's t -test and multiple comparisons done via ANOVA plus *post hoc* Holm-Sidak testing. For KCl induced SD in slice culture, the acquired data was binary (i.e., SD elicited *vs.* no SD elicited) and thus analyzed via Fisher's exact test.

Electrophysiological data was transferred from Axon Instruments software to OriginPro (ver. 8.1; OriginLab) for conversion into manuscript figures. In addition, CorelDRAW X3 (ver. 13.0; Corel Corporation) and then Photoshop (ver. 9.0.2; Adobe) was used to construct final figure images. If any image manipulation was done to enhance visualization, it was always done equally to control, sham, and experimental images.

Results

Clodronate Liposome-Treatment of Slice Culture Selectively Depleted Microglia

Clodronate, a drug that initiates apoptosis when present in sufficiently high concentrations within a cell, was packaged into artificially prepared bilipid vesicles (liposomes) to allow ample uptake by phagocytic cells (van Rooijen, 1989; Vinet et al., 2012). These clodronate-filled liposomes were applied to naïve 20 days *in vitro* hippocampal slice cultures. Seven

TABLE 1: Sequences of RT-PCR Primers

Gene	GenBank accession #	Primer	Sequence (5'-3')
TNFα	NM_012675.3	F R	ACCACGCTCTTCTGTCTACTGA CTGATGAGAGGGAGCCCATTTG
IL-11	NM_133519.4	F R	GCTGACAAGGCTTCGAGTAG TCTTTAGGGAAGGACCAGCT
CD32	NM_175756.1	F R	CCAAACTCGGAGAGAAGCCT CTTCGGAAGACCTGCATGAGA
CD86	NM_020081.1	F R	GAGCTCTCAGTGATCGCCAA CAAACCTGGGGCTGCGAAAAA
Arg-1	NM_017134.3	F R	TGGACCCTGGGGAACACTAT GTAGCCGGGGTGAATACTGG
CD206	NM_001106123.2	F R	AGTCTGCCTTAACCTGGCAC AGGCACATCACTTTCCGAGG
iNOS	NM_012611.3	F R	AGAGACGCTTCTGAGGTTCC GTTGTTGGGCTGGGAATAGC
TGFβ	NM_031131.1	F R	ACCGCAACAACGCAATCTATG TTCCGTCTCCTTGTTTCAGC
IL-10	NM_012854.2	F R	GCTCAGCACTGCTATGTTGC AATCGATGACAGCGTCGCA
Rpl13a	NM_173340.2	F R	TTGCTTACCTGGGGCGTCT CCTTTTCCTTCCGTTTCTCCTC

days later, slice culture vitality was confirmed via Sytox staining before use in experiments or fixation for immunohistochemistry. To determine the degree of microglial depletion and potential effects on other cell types, treated cultures were stained with Iba1, GFAP, CNPase, and NeuN (Fig. 1A). Quantification of Iba1 staining intensity revealed significant depletion of microglia in treated cultures (0.005 ± 0.00 , $n = 9$) versus untreated controls (1.00 ± 0.01 , $n = 9$) (Fig. 1B). Quantification of staining intensity for all other cell types showed no significant difference following clodronate liposome treatment (Fig. 1B). Thus, clodronate liposome treatment of slice cultures provided a microglia-free slice culture that contained normal levels of neurons, oligodendrocytes and astrocytes, allowing us to proceed with electrophysiology experiments.

Microglia were Necessary for Trans-Synaptically and KCl Evoked Spreading Depression

SD threshold was assessed in clodronate liposome-treated slice cultures (i.e., cultures lacking microglia). Evoked synaptic activity was evaluated in all slice cultures before use. Field potential excitatory post-synaptic responses recorded in the CA3 region (Fig. 1C) were not significantly different between control and clodronate-treated cultures, indicating that clodronate treatment had little or no effect on slice culture excitability. Specifically, average post synaptic field potential amplitude for control cultures was (7.50 ± 0.75 mV, $n = 12$) and (6.00 ± 0.51 mV, $n = 12$) for clodronate treated cultures (Fig. 1Ci and Cii, respectively). Next, SD threshold was determined in these cultures by trans-synaptic stimulation as illustrated in Fig. 1Ciii. Trans-synaptically induced SD

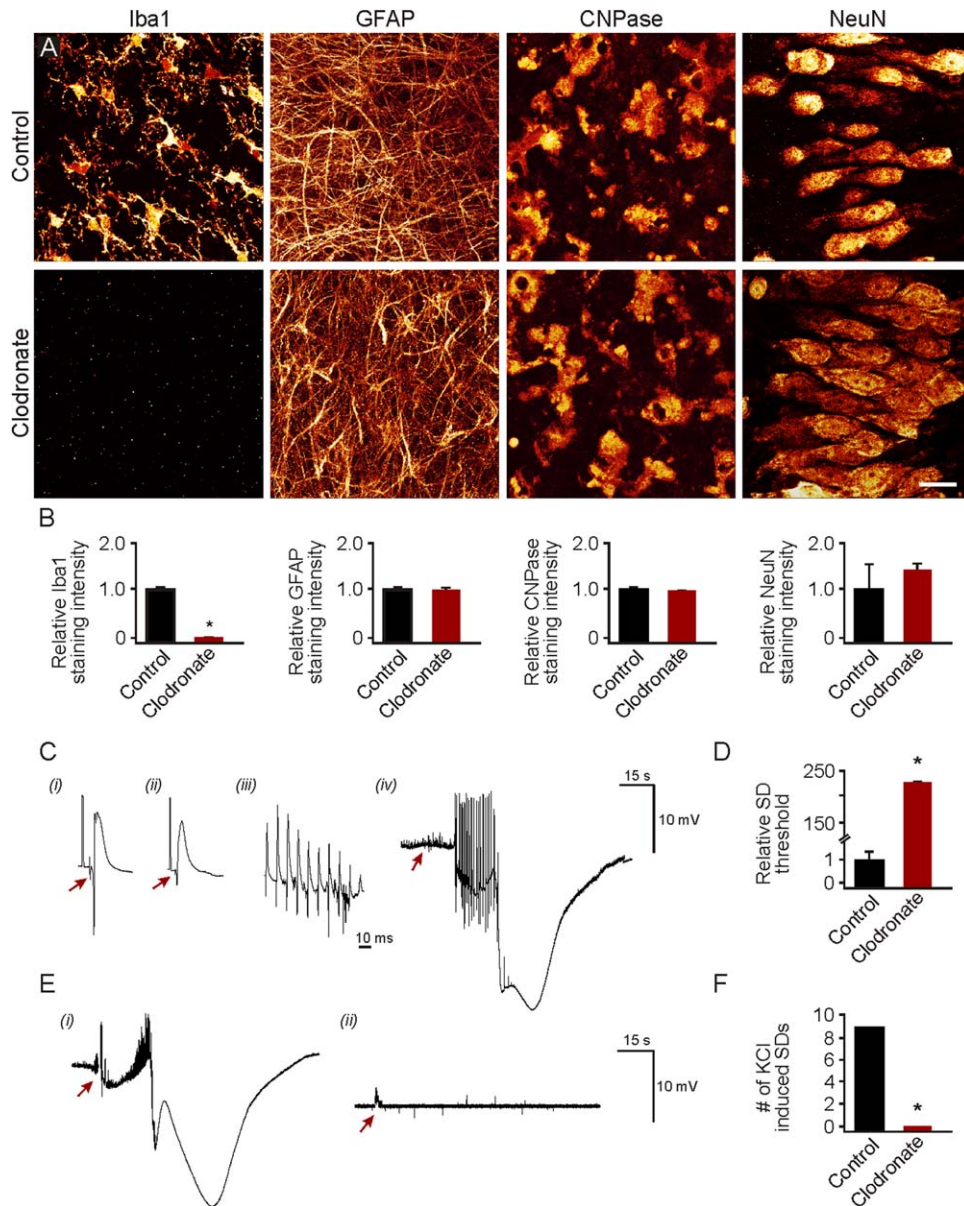


FIGURE 1: Microglia are essential for spreading depression. Slice cultures were treated with clodronate liposomes and stained to assess microglial depletion. (A) Representative staining with cell-specific markers for microglia, astrocytes, oligodendrocytes and neurons (Iba1, GFAP, CNPase, and NeuN, respectively) showed depletion of microglia in clodronate liposome-treated slices (bottom) versus control (top), with no effect on other cell types. Scale bar, 20 μ m. (B) Quantification of cell-specific staining intensity for microglia, astrocytes, oligodendrocytes and neurons. A significant ($*P < 0.001$) decrease in Iba1 staining was seen in clodronate liposome-treated slices. No significant differences were seen in any other cell-specific stains. (C) Representative electrophysiological records are shown for (i) normal field potential, illustrating an initial 10 mV \times 2 ms calibration pulse followed by a stimulation pulse (first negative deflection, indicated by arrow). (ii) Similarly, representative evoked CA3 area field potential response from a slice culture depleted of microglia by clodronate exposure. (iii) 10 Hz stimulation used to trans-synaptically induce SD [with time scale bar applicable to (i, ii, and iii)], and (iv) SD evoked seconds after the electrical stimulation (indicated by arrow). (D) SD threshold was determined for control versus clodronate liposome-treated slices. Depletion of microglia significantly ($*P < 0.001$) increased trans-synaptically induced SD threshold compared with untreated control. In fact, SD was not elicited in treated cultures, but is categorized with the highest current stimulus whether or not it triggered SD. (E) Representative electrophysiological records for (i) KCl-induced SD in control slice cultures and (ii) absence of SD in clodronate liposome-treated slice cultures are shown. Arrows indicate application of KCl stimuli. (F) As with trans-synaptically induced SD, depletion of microglia significantly ($*P < 0.001$) reduced KCl-induction of SD compared with control. In fact, SD was never evoked by KCl in clodronate liposome-treated slice cultures.

threshold was significantly higher in clodronate liposome-treated (227.00 ± 0.00 , $n = 6$) versus untreated control cultures (1.00 ± 0.41 , $n = 6$) (Fig. 1D). However, it is impor-

tant to note that the maximum stimulus used to attempt induction of SD was 10,000 nC. This amount of current was unable to evoke SD in any microglia depleted cultures, but

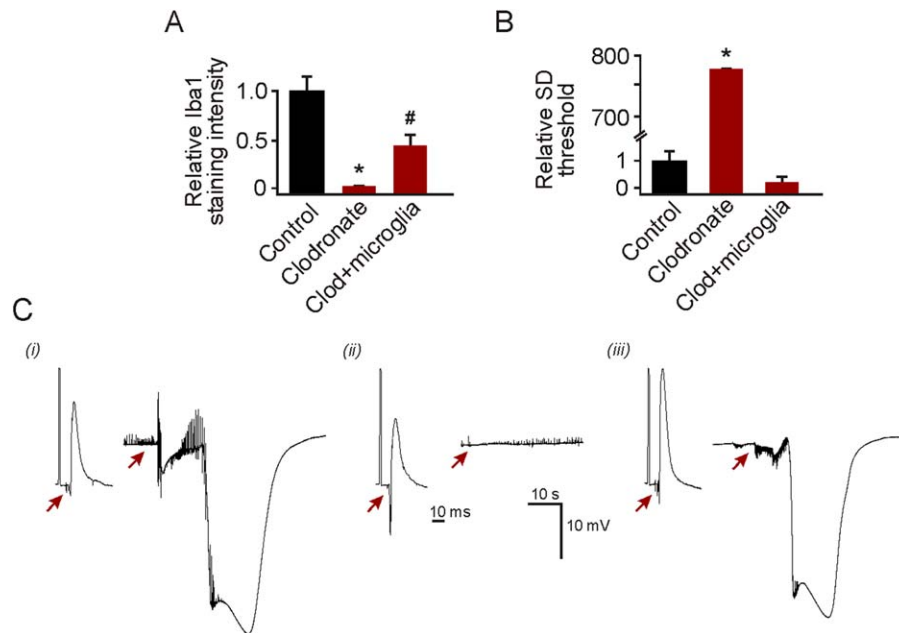


FIGURE 2: Restoration of microglia to previously depleted cultures reestablished their susceptibility to spreading depression. Slice cultures were treated with clodronate liposomes as before, and supplemented with cultured primary microglia. (A) Quantification of Iba1 staining intensity for microglia. A significant ($*P < 0.001$) decrease in Iba1 staining was seen in clodronate treated cultures, whereas Iba1 staining in clodronate + microglia treated cultures was significantly ($\#P < 0.001$) improved toward normal levels. (B) SD threshold was determined for control versus clodronate liposome-treated and clodronate + microglia treated cultures. Depletion of microglia significantly ($*P < 0.001$) increased trans-synaptically induced SD threshold compared with untreated control, whereas addition of exogenous microglia re-established the ability to evoke SD toward control levels. (C) Representative electrophysiological records (field potential to left and SD (if elicited to right) for (i) control, (ii) clodronate-treated, and (iii) clodronate + microglia treated slice cultures. Once again, SD was induced in control cultures but not in clodronate-treated cultures. Importantly, clodronate-treated cultures supplemented with microglia showed markedly increased evoked excitability of SD ($n = 5$), seizures ($n = 2$), and bursting ($n = 1$) to single electrical pulses.

our statistical analysis scaled this value relative to the SD threshold nC of untreated controls.

SD was also induced by transient contact of a 1M KCl-agar filled wand to the dentate gyrus (Fig. 1E*d*). In all instances, KCl promptly induced SD ($n = 9$) in untreated cultures, while similar KCl application to the dentate gyrus of clodronate liposome-treated slice cultures never induced SD ($n = 9$) (Fig. 1E*ii*). Thus, microglia were essential for initial induction of SD in hippocampal slice cultures, a model which closely mimics conditions found in the *in vivo* counterpart.

Notably, our SD results were not consistent with “spreading depolarizations” (i.e., depolarizations that spread with the absence of preceding spontaneous activity; Dreier et al., 2011). All of our brain slice cultures showed spontaneous neuronal activity before SD stimulation (see Fig. 1C*iv*, Fig. 1E*ii*; the relative thickness of the DC recording is due to overlying activity, whereas the recording becomes a thin line in the absence of this activity during SD).

Restoration of Microglia to Previously Depleted Cultures Reestablished Their Susceptibility to Spreading Depression

To confirm the presence of exogenously added microglia, clodronate-treated, microglia-supplemented cultures were

stained with Iba1. Quantification of Iba1 staining intensity again confirmed significant depletion of microglia in clodronate treated cultures (0.01 ± 0.00 , $n = 6$) versus untreated controls (1.00 ± 0.06 , $n = 6$), and revealed significant restoration of microglia in supplemented cultures (0.45 ± 0.12 , $n = 6$) (Fig. 2A). However, single evoked stimuli to the dentate gyrus of clodronate-treated, microglia-supplemented cultures provoked hyperexcitable responses that precluded accurate measurement of post synaptic field response amplitude. Trans-synaptically induced SD threshold was significantly higher in clodronate-treated (777.00 ± 0.00 , $n = 6$) versus untreated control cultures (1.00 ± 0.37 , $n = 6$), whereas SD threshold in clodronate-treated cultures supplemented with primary microglia were not significantly different from controls (0.20 ± 0.20 , $n = 5$) (Fig. 2B). Representative electrophysiological records for each group are shown in Fig. 2C. Field potential excitatory post-synaptic amplitudes for control and clodronate-treated cultures were consistent with those reported above (Fig. 1), while those for clodronate-treated microglia-supplemented cultures tended to be larger and occasionally triggered bursting or seizure activity ($n = 3$), which precluded induction of SD.

Environmental Enrichment of Animals Increased Spreading Depression Threshold and Decreased Baseline Oxidative Stress

EE is well-known to improve the outcome of neurological diseases, including but not limited to migraine. Furthermore, EE reduces the propagation velocity of SD (Gueddes et al., 1996). Accordingly, we determined SD threshold in rats exposed to EE compared with NE age-matched controls by recording KCl-induced SD (Fig. 3A). Whole animal neocortical SD threshold was significantly increased by EE (9.82 ± 0.75 , $n = 5$) compared with NE counterparts (1.00 ± 0.26 , $n = 6$) (Fig. 3B). Protein carbonyl levels were also measured in naïve EE versus NE rat neocortex, as a means to assess differences in baseline levels of OS. We found a significant decrease in carbonylated protein content in EE neocortex (7.10 ± 0.29 nmol/mg, $n = 3$) compared with NE neocortex (11.90 ± 1.15 nmol/mg, $n = 3$) (Fig. 3C). This further supports the ability of EE to mitigate SD (and by extension, migraine), and suggests that reduction of OS may be involved in this effect.

Environmental Enrichment Increased CNS Levels of IL-11

Since IL-11 reduces TNF α (Mitchell et al., 2011) which is an important stimulus for the generation of microglial ROS following SD (Grinberg et al., 2013), we determined IL-11 and TNF α expression levels in EE and NE brains via semi-quantitative RT-PCR. IL-11 mRNA expression was significantly higher in EE versus NE brains (10.6 fold), whereas TNF α mRNA levels were not significantly different (<2-fold) (Fig. 3D). To confirm this increase in IL-11 mRNA, we next stained for IL-11 protein in EE and NE brains. Double-staining with NeuN indicated that neuronal IL-11 was increased in EE (Fig. 3E; right) relative to NE brains (Fig. 3E; left). Thus, EE increased CNS levels of IL-11, which may contribute to the observed reduction in OS and SD (detailed above).

M2a Polarization of Microglia led to Increased Spreading Depression Threshold

To determine the relative contribution of pro-inflammatory M1 microglia to induction of SD, we inhibited signaling from classically activated microglia (effectively creating an M2a-biased phenotype) via application of minocycline. Minocycline was used at 10 μ M, a dose that inhibits microglial function (Hulse et al., 2008). Minocycline selectively inhibits M1 activation—thus reducing production of inflammatory molecules including TNF α and iNOS—while not affecting M2a polarization (Kobayashi et al., 2013). Application of minocycline significantly increased SD threshold (13.20 ± 5.53 , $n = 3$) compared with untreated control (1.00 ± 0.33 , $n = 9$) slice cultures (Fig. 4A). Likewise, application of exog-

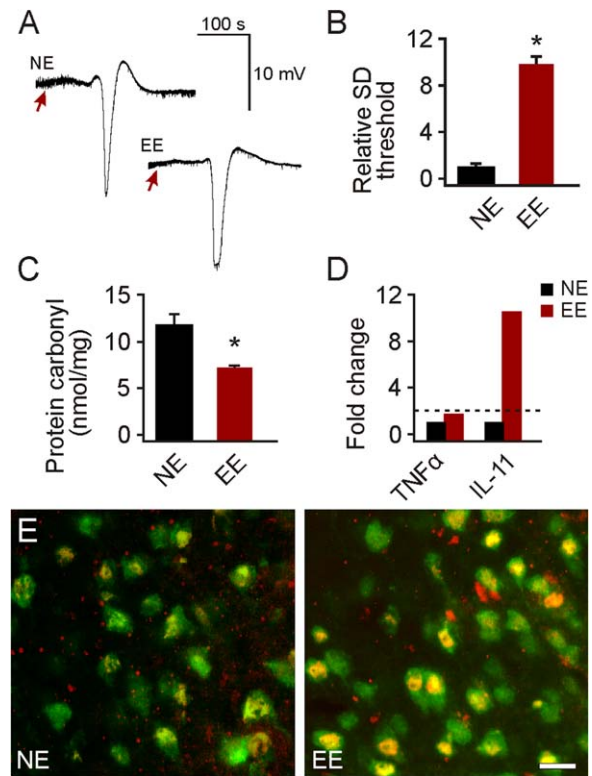


FIGURE 3: Environmental enrichment increases IL-11 and spreading depression threshold. (A) Representative electrophysiological records are shown for KCl-induced whole animal neocortical spreading depression (SD) from environmentally enriched (EE) and non-enriched (NE) animals. (B) Whole animal SD threshold was determined for NE and EE rats. EE animals showed a significantly ($*P < 0.001$) increased SD threshold compared with NE animals. (C) Protein carbonyl content was measured in NE and EE neocortex. EE brains contained significantly ($*P = 0.016$) lower levels of carbonylated protein relative to NE controls. (D) Semiquantitative RT-PCR shows no increase (<2-fold) in TNF α mRNA in EE versus NE brains, whereas increased expression (10.6-fold) was seen in IL-11 mRNA. (E) Representative images of rat brain sections (40 μ m) double-stained for IL-11 (red) and NeuN (green) show increased neuronal IL-11 (yellow) in neocortex of EE versus NE animals. Scale bar, 20 μ m.

enous IL-11 to mimic the increase of IL-11 seen in EE brains also increased SD threshold (120.00 ± 23.00 , $n = 8$) relative to control (1.00 ± 0.34 , $n = 6$) slice cultures (Fig. 4B). Since reduction of M1 polarization and exogenous IL-11 both increased SD threshold, we next looked to determine if IL-11 could shift microglial polarization to an M2a dominant phenotype. IL-11 was applied to primary microglial cultures, and immunohistochemistry for M1 and M2a markers (CD32 and Arg-1 respectively) was performed (Fig. 4C). Quantification of staining intensity revealed a significant increase in M2a (Arg-1 positive staining) in IL-11-treated microglia cultures (1.07 ± 0.01 , $n = 3$) compared with untreated cultures (1.00 ± 0.01 , $n = 3$) (Fig. 4D). Staining for M1 and M2a markers was also performed in IL-11 treated slice cultures to

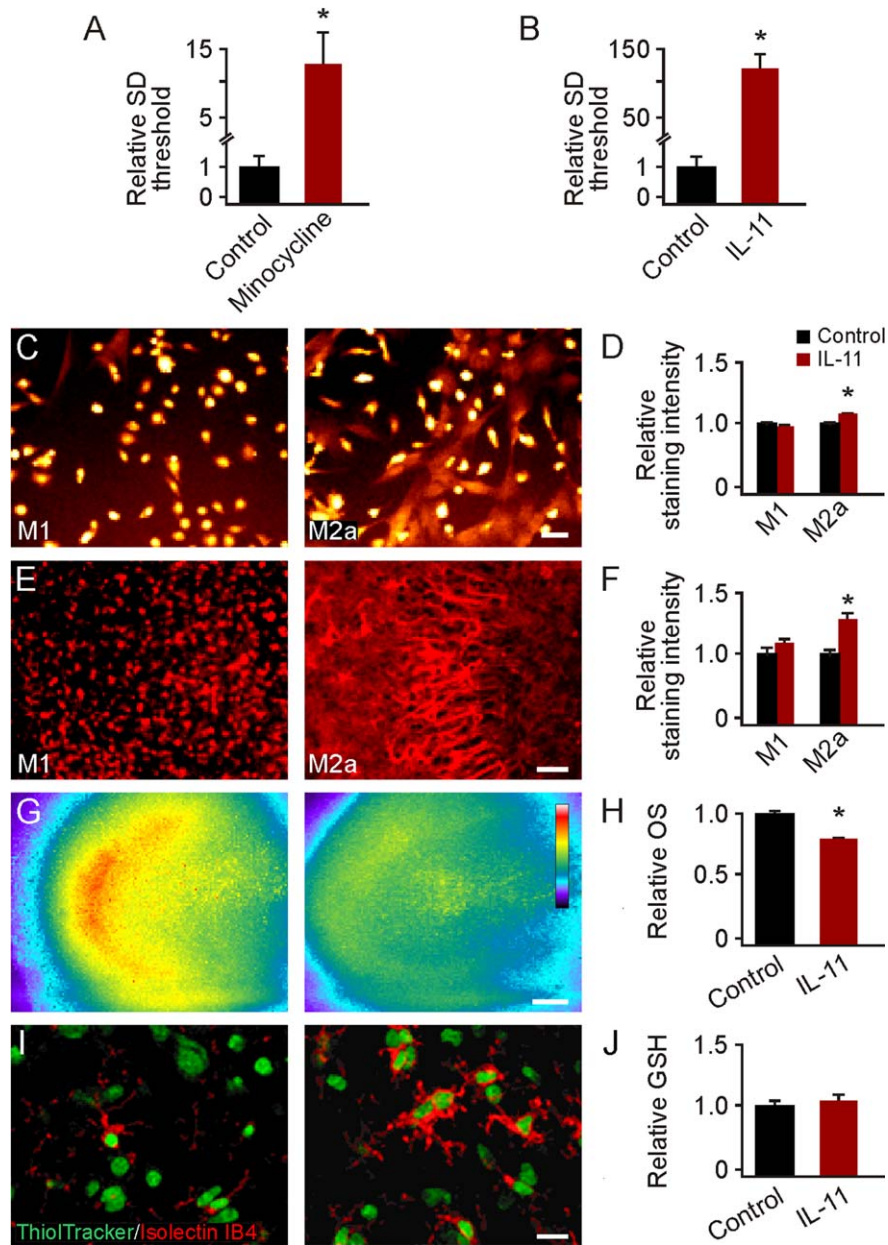


FIGURE 4: Pharmacological induction of microglial M2a phenotype occurs with increased spreading depression threshold. Trans-synaptically induced spreading depression (SD) threshold was significantly increased in both (A) minocycline-treated slice cultures ($*P < 0.002$) and (B) IL-11-treated slice cultures ($*P < 0.001$) versus untreated controls. (C) Representative images of M1 (CD32) and M2a (Arg-1) staining of IL-11-treated primary microglia cultures. Scale bar, 20 μm . (D) Quantification of M1 and M2a staining intensities show a significant ($*P = 0.008$) increase in M2a-specific staining in IL-11-treated primary microglia cultures. (E) Representative images of M1 (CD32) and M2a (Arg-1) staining of IL-11-treated hippocampal slice cultures. Scale bar, 20 μm . (F) Quantification of M1 and M2a staining intensities show a significant ($*P = 0.008$) increase in M2a-specific staining of microglia in IL-11-treated slice cultures. (G) Representative images of staining for menadione-induced oxidative stress (CellROX) in control (left) and IL-11-treated (right) slices. Scale bar, 200 μm . (H) Quantification of CellROX fluorescence intensity at the CA3 region shows a significant ($*P = 0.005$) decrease in oxidative stress in IL-11-treated versus untreated controls. (I) Representative images of ThiolTracker [green; glutathione (GSH)] and Isolectin-IB4 (red; microglia) double-staining in control (left) and IL-11-treated (right) slices. Scale bar, 20 μm . (J) Quantification of ThiolTracker fluorescence intensity showed no significant difference in glutathione levels between control and IL-11-treated slices.

determine polarization of microglia in the presence of neural tissue maintained *in vitro* (Fig. 4E). As with primary microglia cultures, application of IL-11 to slice cultures significantly increased M2a polarization of microglia (1.28 ± 0.08 ,

$n = 5$) compared with untreated cultures (1.00 ± 0.04 , $n = 5$) (Fig. 4F). Since we observed increased IL-11 in conjunction with decreased OS in whole animals exposed to EE (Fig. 2), we next assessed the impact of IL-11 on OS. IL-11 was

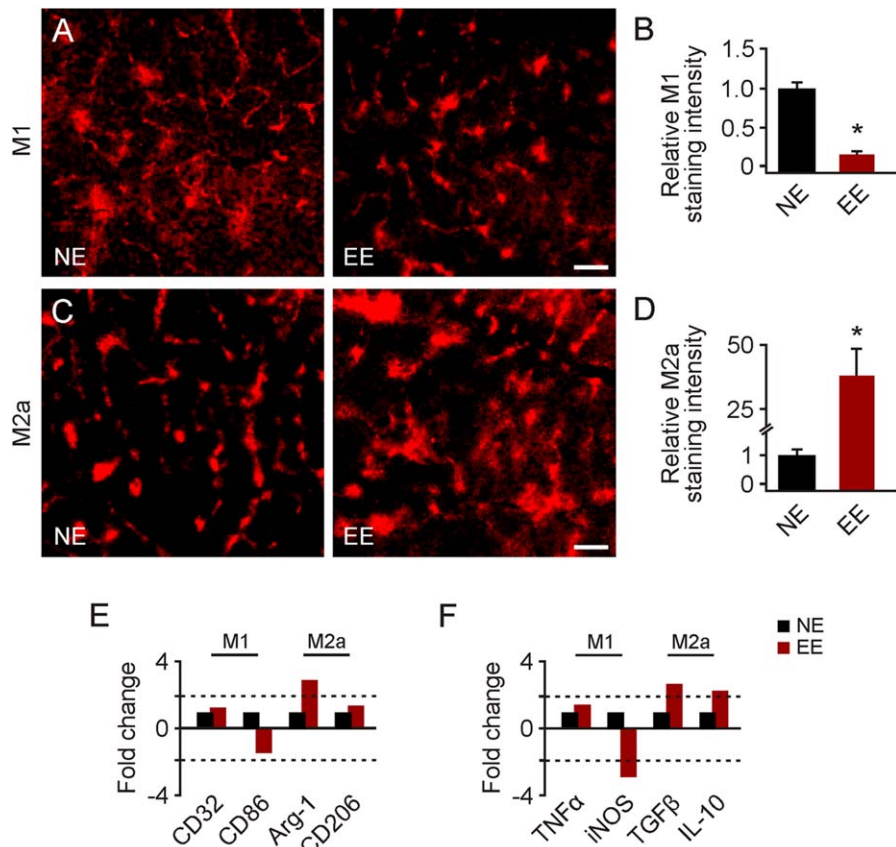


FIGURE 5: Environmental enrichment drives microglia to M2a phenotype. Immunostaining of nonenriched (NE) and environmentally enriched (EE) brain sections (40 μ m) for M1 and M2a specific markers (CD32 and Arg-1, respectively). (A) Representative images of CD32 staining in NE and EE neocortex. Scale bar, 20 μ m. (B) Quantification of CD32 staining intensity shows significantly ($*P < 0.001$) reduced M1 microglia/macrophages in EE versus NE. (C) Representative images of Arg-1 staining in NE and EE neocortex. Scale bar, 20 μ m. (D) Quantification of Arg-1 staining intensity shows significantly ($*P = 0.021$) increased M2a microglia/macrophages in EE versus NE. Semi-quantitative RT-PCR was performed for M1 and M2a gene expression. (E) Assessment of classical M1 and M2a surface markers showed increased (2.9-fold) expression of Arg-1 mRNA (M2a) in EE versus NE. M1 markers (CD32 and CD86) showed similar or slightly reduced (<2-fold) expression levels in EE versus NE. (F) Assessment of select mRNAs indicative of M1 versus M2a polarization showed increased expression of M2a-specific TGF β and IL-10 mRNA (2.7- and 2.4-fold, respectively), and reduced expression (3.0-fold) of M1-specific iNOS mRNA. Expression levels of M1-specific TNF α mRNA were not significantly different (<2-fold).

applied to slice cultures for three days before induction of OS via menadione treatment. CellROX was used as a means to assess OS (Fig. 4G; control: left, IL-11 treatment: right). Pre-treatment with IL-11 significantly decreased slice culture OS (0.81 ± 0.03 , $n = 9$) compared with that seen in untreated controls (1.00 ± 0.05 , $n = 9$) (Fig. 4H). Prior work has implicated microglial production of glutathione as a key component of antioxidant defense mechanisms in the CNS (Dringen, 2005). Thus, we performed double staining of ThiolTracker and Isolectin-IB4 in control (Fig. 4I; left) versus IL-11-treated (Fig. 4I; right) slices to determine changes in microglial glutathione levels. However, no significant difference was seen between the two groups (Fig. 4J). This begins to suggest that the observed decrease in OS may be due to decreased production of reactive oxygen or nitrogen species, rather than a specific upregulation of antioxidants.

Environmental Enrichment Induced a Shift Toward an M2a Phenotype

Since IL-11 increased M2a polarization in primary microglial cultures, and IL-11 was significantly increased in EE brains, we next looked at microglial polarization in EE versus NE brains. Staining for M1-specific marker CD32 (Fig. 5A; NE: left, EE: right) showed a significant reduction of M1 polarization of microglia/macrophages in neocortex of EE (0.14 ± 0.03 , $n = 3$) versus NE (1.00 ± 0.09 , $n = 3$) animals (Fig. 5B). In contrast, staining for M2a-specific marker Arg-1 (Fig. 5C; NE: left, EE: right) revealed a significant increase in M2a polarization in EE (38.00 ± 10.00 , $n = 3$) compared with NE (1.00 ± 0.25 , $n = 3$) neocortex (Fig. 5D). To confirm immunohistochemistry assessment of protein levels, semi-quantitative RT-PCR was performed for M1 and M2a gene expression. M1 polarization was determined by

expression levels of surface protein markers CD32 and CD86, as well as M1 products TNF α and iNOS. M2a polarization was determined by expression levels of surface protein markers Arg-1 and CD206, as well as M2a products TGF β and IL-10. A significant increase (2.9-fold) was found in Arg-1 mRNA expression in EE *versus* NE brains, though no significant change (<2-fold) was seen in M1-specific CD32 and CD86 or M2a-specific CD206 (Fig. 5E). Furthermore, expression of M2a products TGF β and IL-10 were significantly higher in EE (2.7-fold and 2.4-fold, respectively) compared with NE brains, whereas expression of M1 product iNOS was significantly reduced (3.0-fold). No significant change was observed in TNF α mRNA levels (Fig. 5F). Taken together, this gene expression data indicate a shift of microglia/macrophages toward an M2a phenotype in EE animals. Though M1 surface markers and TNF α were not significantly changed, it is notable that iNOS (a producer of reactive nitrogen species) was significantly reduced.

M2a Microglia Conditioned Medium Increased Spreading Depression Threshold While Maintaining Normal Levels of Oxidative Stress

To further confirm whether M1 and M2a microglia alter SD threshold through changes in the local environment (i.e., the inflammatory and oxidative state of the brain) via secreted agents, we applied conditioned medium from polarized primary microglia to slice cultures. Primary microglial cultures (Fig. 6A,B, left) were polarized to an M1 phenotype by application of LPS (Fig. 6A, right), or to an M2a phenotype via application of IL-4 (Fig. 6B, right). Naïve slice cultures were incubated in M1 or M2a conditioned media, and SD threshold determined three days later. Exposure to M2a conditioned medium significantly increased SD threshold (349.50 ± 107.80 , $n = 8$) relative to M1 conditioned medium exposure (1.03 ± 0.33 , $n = 9$) and control (1.00 ± 0.31 , $n = 9$) (Fig. 6C).

OS levels were also measured following exposure to conditioned media. Slice cultures incubated in M1 conditioned medium, M2a conditioned medium, or normal serum-free medium were exposed to menadione as above, and OS measured via CellROX (Fig. 7A). A significant increase was seen in slices exposed to M1 conditioned medium (1.33 ± 0.09 , $n = 5$), indicating production of reactive oxygen/nitrogen species above that induced by menadione alone. However, quantification of CellROX fluorescence intensity showed no significant decrease in OS from menadione in cultures treated with M2a conditioned medium (1.10 ± 0.09 , $n = 5$) compared with cultures exposed to menadione alone (1.0 ± 0.05 , $n = 6$). This suggests a lack of increased antioxidant production in the latter condition (Fig. 7B).

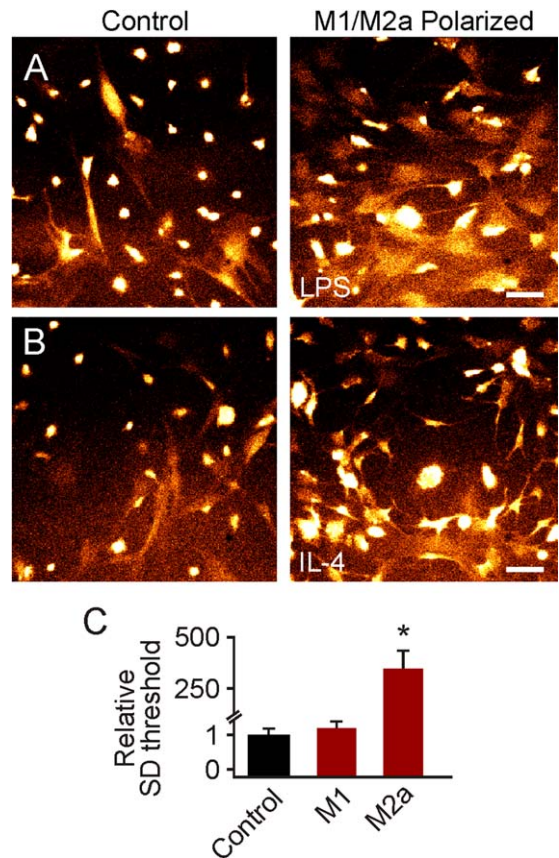


FIGURE 6: M2a microglia-conditioned medium increases spreading depression threshold. Primary microglia cultures were polarized to an M1 (treated with 1 μ g/mL LPS) or M2a (treated with 20 ng/mL IL-4) phenotype. (A) Representative images of CD32 staining of untreated (left) and LPS-treated (right) primary microglia cultures show increased CD32 positive staining in treated cultures. Scale bar, 200 μ m. (B) Representative images of Arg-1 staining of untreated (left) and IL-4-treated (right) primary microglia cultures show increased Arg-1 positive staining in treated cultures. Scale bar, 20 μ m. (C) Naïve hippocampal slice cultures were incubated in conditioned medium derived from M1 or M2a polarized microglia cultures, and spreading depression (SD) threshold determined three days later. Trans-synaptically induced SD threshold was significantly (* $P < 0.001$) increased in hippocampal slices treated with M2a-conditioned medium *versus* those treated with M1-conditioned medium and untreated control slice cultures.

Nasal Administration of IL-11 Mimicked Environmental Enrichment by Promoting an M2a Phenotype

Since EE animals had increased IL-11, and IL-11 both alters microglial polarization and protects from SD in slice cultures, we next administered IL-11 to whole animals to determine its efficacy *in vivo*. Naïve rats were nasally administered IL-11 (1 mg) or sodium succinate buffer alone (sham), and used 1 day later for measurement of all variables assessed in EE animals (Fig. 4).

Whole animal SD threshold determination revealed significantly increased threshold in IL-11-treated (24.40 ± 8.90 ,

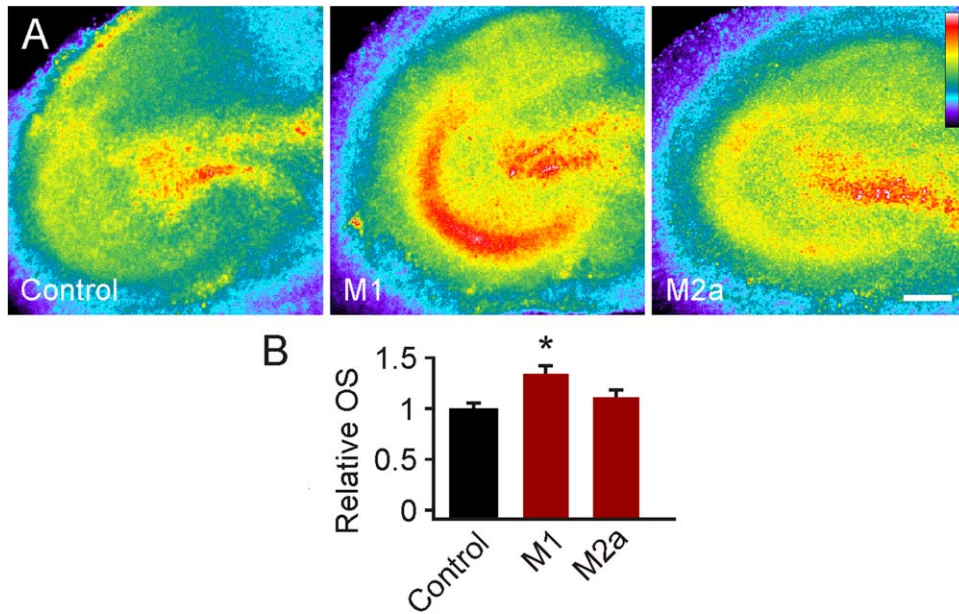


FIGURE 7: M1 microglia-conditioned medium increases oxidative stress. Naïve slice cultures were incubated in conditioned medium derived from M1 or M2a polarized primary microglia cultures. (A) Representative images of staining for menadione-induced oxidative stress (OS; CellROX) in control (left), M1 conditioned medium-treated (middle) and M2a conditioned medium-treated (right) hippocampal slice cultures. Scale bar, 200 μ m. (B) Quantification of CellROX fluorescence intensity at the CA3 region showed a significant ($*P = 0.006$) increase of OS in hippocampal slices treated with M1 conditioned medium versus slices treated with M2a conditioned medium or menadione alone (control).

$n = 5$) versus sham (1.00 ± 0.14 , $n = 5$) animals (Fig. 8A). As in EE animals, baseline protein carbonyl content was also significantly lower in IL-11 treated (7.29 ± 1.69 nmol/mg, $n = 3$) versus sham (13.89 ± 0.39 nmol/mg, $n = 3$) animals (Fig. 8B).

Staining for M1-specific marker CD32 (Fig. 8C; left and middle) showed no significant difference in M1 polarization of microglia/macrophages in neocortex of rats nasally administered IL-11 (1.06 ± 0.05 , $n = 3$) versus shams (1.00 ± 0.05 , $n = 3$) (Fig. 8C; right). In contrast, staining for M2a-specific marker Arg-1 (Fig. 8D; left and middle) revealed a significant increase in M2a polarization in IL-11-treated (1.21 ± 0.04 , $n = 3$) compared with sham (1.00 ± 0.04 , $n = 3$) neocortex (Fig. 8D; right). As above, semiquantitative RT-PCR was performed for M1 and M2a gene expression. mRNA expression was significantly increased (4.4 fold) for CD206 and decreased (2.3 fold) for CD86 in IL-11-treated versus sham brains. No significant changes (<2-fold) in CD32 or Arg-1 were seen (Fig. 8E). Expression of IL-10 was significantly higher in IL-11-treated animals (2.1-fold), though TGF β was just under significance (1.7-fold) compared with sham brain levels. Expression of iNOS was significantly reduced (2.3-fold) and no significant change was observed in TNF α levels (Fig. 8F). Once again, this gene expression data indicated a shift of microglia/macrophages towards an M2a phenotype in IL-11-treated animals, similar

to that seen in EE animals (Fig. 4). Thus, IL-11 mimicked the effects of EE.

Discussion

Previous studies by our laboratory have demonstrated that microglial TNF α and OS play an important role in increasing susceptibility to SD after recurrent SD (Grinberg et al., 2012, 2013). Here, we show that microglia are also instrumental in triggering an *initial* event of SD by ablating microglia in hippocampal slice cultures through application of clodronate liposomes. Using this method, we were able to selectively deplete microglia without adversely affecting levels of other cell types. Furthermore, clodronate treatment did not affect slice culture evoked neuronal activity, as assessed by presence of normal field potential excitatory post-synaptic responses. This allowed us to perform electrophysiological experiments in slices with intact neuronal/synaptic activity to determine the threshold for evoking SD with and without microglia. In the absence of microglia we were unable to initiate SD (Fig. 1D,F). Though we cannot delineate whether this was directly due to the lack of microglia, or indirectly via neighboring cells, adding primary microglia back to depleted cultures restored the ability to evoke SD (Fig. 2C). This suggests that in addition to being a critical component of enhancing susceptibility after

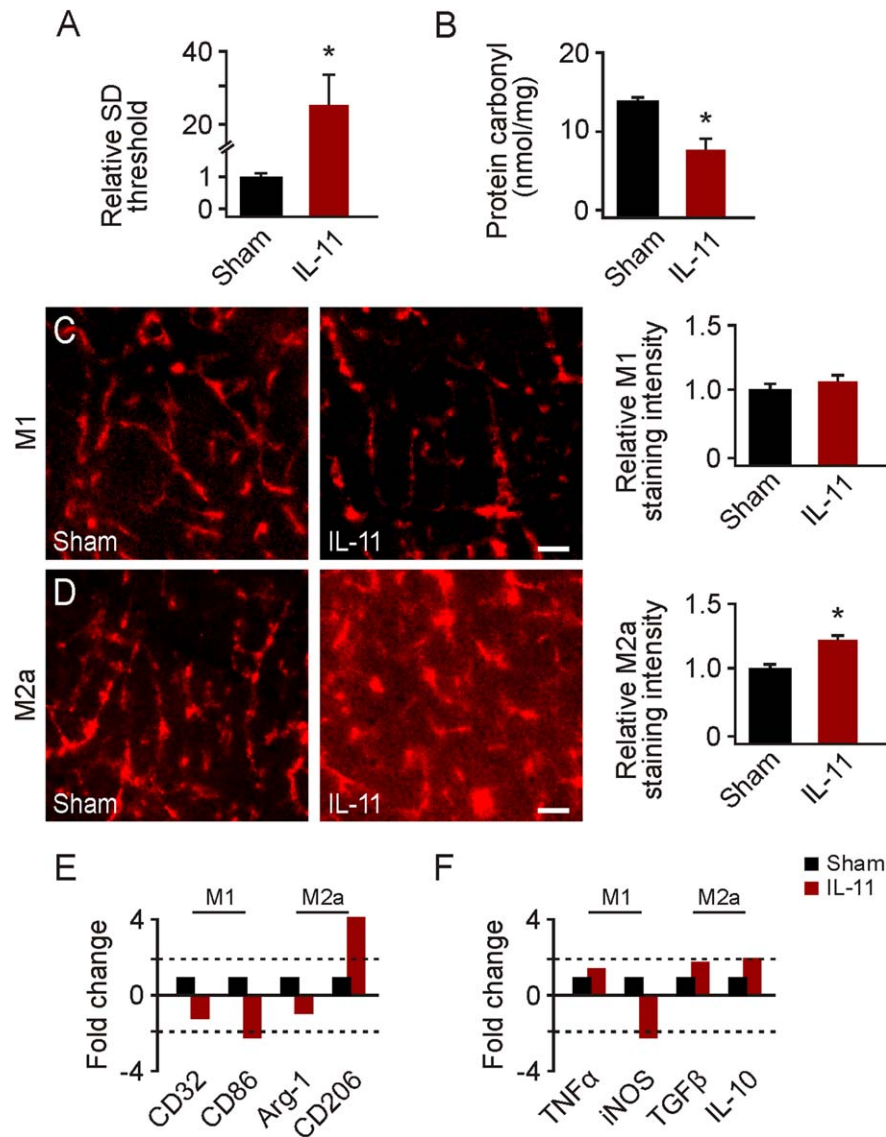


FIGURE 8: Nasal administration of IL-11 mimics environmental enrichment. Animals were nasally administered IL-11 (1 mg) or sodium succinate alone (sham). All measurements were taken 1 day post-treatment. (A) Whole animal spreading depression (SD) threshold was determined for IL-11-treated and sham rats. Nasal administration of IL-11 significantly ($*P = 0.03$) increased SD threshold compared with sham. (B) Assessment of protein carbonyl levels was performed as a measure of oxidative stress. Animals that were nasally administered IL-11 exhibited significantly ($*P = 0.02$) lower levels of carbonylated protein. Immunostaining of IL-11-treated and sham brain sections (40 μm) for M1 and M2a specific markers (CD32 and Arg-1, respectively). (C) Representative images of CD32 staining in neocortex of sham and IL-11-treated animals. Scale bar, 20 μm . Quantification of CD32 staining intensity showed no significant difference in M1 microglia/macrophages between sham and IL-11-treated animals. (D) Representative images of Arg-1 staining in neocortex of sham and IL-11-treated animals. Scale bar, 20 μm . Quantification of Arg-1 staining intensity showed significantly ($*P = 0.014$) increased M2a microglia/macrophages in IL-11-treated versus sham animals. Semi-quantitative RT-PCR was performed for M1 and M2a gene expression. (E) Assessment of classical M1 and M2a surface markers showed increased (4.4-fold) expression of CD206 mRNA (M2a) and reduced (2.3-fold) expression of CD86 mRNA (M1) in IL-11-treated versus sham animals. Expression of CD32 and Arg-1 mRNA was not significantly different (<2 -fold). (F) Assessment of select mRNAs indicative of M1 versus M2a polarization showed increased expression of M2a-specific IL-10 mRNA (2.1-fold), and reduced expression (2.3-fold) of M1-specific iNOS mRNA. Expression levels of M2a-specific TGF β and M1-specific TNF α mRNA were not significantly different (<2 -fold).

recurrent SD (Grinberg et al., 2012, 2013), microglia are also necessary for evoking *initial* SD itself.

A sufficient volume of grey matter must be synchronously depolarized above a threshold to initiate SD in susceptible brain regions. This threshold level of depolarization has

long been recognized to involve adequate elevations of interstitial potassium and glutamate (Bureš et al., 1974; Somjen, 2001). Astrocytes are macroglia that help regulate interstitial homeostasis. Thus their role in SD initiation has been extensively documented (for review see Grafstein, 2011;

Martins-Ferreira et al., 2000). Microglia, on the other hand, are only recently recognized as key regulators of neuronal excitability via their involvement in potassium and glutamate homeostasis. Additionally, microglial immune signaling can further increase excitability by amplifying traditional electrophysiological signaling (Devinsky et al., 2013; Pusic et al., 2011; Rodriguez et al., 2013). Our work adds to the growing literature indicating that microglia are instrumental in mitigating hyperexcitability caused by inflammation, and that EE-induced changes in microglia may be an important part of this process.

Since EE is a natural therapeutic option shown to reduce migraine frequency (Darabaneanu et al., 2011), and recent work suggests that EE dampens pro-inflammatory responses from microglia and astrocytes (Williamson et al., 2012), we next asked whether this reduction of pro-inflammatory signaling affects SD threshold. Here, it is important to note that while prior studies have shown that the effects of voluntary exercise and those from exposure to an enriched environment are separable (Olson et al., 2006), they provide the greatest benefit when used simultaneously (Fabel et al., 2009).

Our study found that whole animals exposed to EE had significantly higher SD thresholds than age-matched NE animals (Fig. 3B). Examination of EE *versus* NE brains also revealed significantly reduced protein carbonylation, a measure of oxidative stress, in EE neocortex (Fig. 3C). This may indicate either decreased ROS production or increased antioxidant capacity, both of which would decrease net OS, which is a key component of SD initiation. This baseline decrease in OS may also be a key mechanism of EE-induced neuroprotection in a number of other disease models where pro-oxidants initiate or exacerbate damage, such as stroke, seizure, and neurodegenerative disorders.

We next examined levels of IL-11, an anti-inflammatory cytokine with known immunomodulatory and neuroprotective properties (Maheshwari et al., 2013; Trepicchio and Dorner, 1998; Trepicchio et al., 1996; Zhang et al., 2006). Semiquantitative RT-PCR measurement of IL-11 mRNA revealed an increase in IL-11 expression, as well as an expected reduction in TNF α expression in EE *versus* NE brains (Fig. 3D). Interestingly, double staining for IL-11 and NeuN in sectioned neocortex suggests increased IL-11 production by neurons in EE exposed animals (Fig. 3E). Taken together, these data suggest that EE mitigation of migraine involves dampening of pro-inflammatory signaling and resultant OS. Furthermore, the observed increase in IL-11 levels, which correlate with physically increased neuronal activity from learning associated with EE (van Praag et al., 2000), may contribute to this effect.

Microglial M1 polarization is associated with increased production of pro-inflammatory cytokines and reactive oxy-

gen/nitrogen species (Ajmone-Cat et al., 2013; Durafourt et al., 2012). To determine whether decreasing this pro-inflammatory signaling mitigates SD, and thus perhaps migraine, we applied minocycline to slice cultures and measured SD threshold. Minocycline is a tetracycline antibiotic that selectively inhibits M1 polarized microglia, thus reducing production of pro-inflammatory cytokines (Kobayashi et al., 2013). Treatment with minocycline significantly increased SD threshold (Fig. 4A), indicating that M1 polarization contributes to induction of SD. Decreasing pro-inflammatory signaling through application of exogenous IL-11 likewise increased SD threshold (Fig. 4B), supporting the idea that increased IL-11 from EE protects from migraine. We next wanted to determine the effects of IL-11 on microglial polarization and slice culture OS. Exposure to IL-11 produced an M2a-skewed phenotype in both primary microglial cultures and hippocampal slice cultures (Fig. 4C–F), and IL-11 treatment significantly decreased OS from menadione exposure in slice culture (Fig. 4G,H). However, slice culture treatment with IL-11 did not increase microglial glutathione content (Fig. 4I,J). This suggests that IL-11 increases SD threshold by dampening M1 polarization and therefore reducing M1-associated inflammatory and pro-oxidant effects.

Since IL-11 shifted microglia to an M2a dominant phenotype, we next looked to M2a polarization in EE brains as a potential mechanism for abrogation of SD. We assessed M1 and M2a polarization using a combination of immunohistochemical staining for known M1 *versus* M2a surface markers and semi-quantitative RT-PCR of additional markers and products. Animals exposed to EE had significantly lower M1 and higher M2a levels compared with NE animals, further supporting the role of reduced inflammation in EE mitigation of migraine (Fig. 5).

We next sought to determine if microglia polarization to an M2a *versus* M1 dominated phenotype creates an environment of decreased OS that in turn reduces SD. By doing so, we could also affirm that the effect we observe from EE and IL-11 are mediated by products of microglial activation. M1 conditioned medium had no effect on SD threshold, whereas M2a conditioned medium significantly increased SD threshold above that of control untreated slice cultures (Fig. 6C). However, while M2a conditioned medium had no effect, M1 conditioned medium exacerbated OS following exposure to menadione (Fig. 7).

Finally, we asked whether administration of exogenous IL-11 could mimic the nutritive effects seen from exposure to EE. Nasally delivered cytokines, such as insulin-like growth factor-1 (IGF-1), have been shown to rapidly diffuse via bulk flow along olfactory and trigeminal nerves before being distributed more widely throughout the brain (Liu et al., 2001; Lockhead and Thorne, 2012; Thorne et al., 2004). SD

threshold was significantly increased in rats nasally administered IL-11 *versus* aged matched controls administered sodium succinate (vehicle) alone (Fig. 8A). Furthermore, these IL-11 treated animals showed a significant decrease in protein carbonylation (Fig. 8B), and exhibited an M2a-skewed phenotype (Fig. 8C–F), measured as before with both immunohistochemistry and semi-quantitative RT-PCR. Thus, nasal administration of IL-11 can closely mimic the M2a polarization and associated reduction of SD seen from exposure to EE.

Interestingly, the significant decrease in protein carbonylation in the neocortex of EE and IL-11-treated rats relative to NE and sham animals was not reflected in increased production of microglial glutathione. Additionally, M2a polarization did not protect from acute menadione exposure, while M1 polarization increased the resultant degree of OS. Taken together, these data begin to suggest that EE protection from SD is mediated not by an increase in antioxidant production from M2a microglia, but a decrease in M1 microglia generation of oxidants and pro-inflammatory cytokines.

Mounting evidence shows that changes in microglial polarization likely impacts downstream nociceptive signaling of migraine, as well as chronic pain (Tsuda et al., 2013). For example, TNF α (a M1 polarization product) induces sensitization of meningeal nociceptors, which play a role in migraine pain signaling (Zhang et al., 2011). Also, neocortical SD induces OS in the trigeminal nociceptive system (Shatillo et al., 2013). It is likely that an M1 dominant phenotype contributes to enhanced migraine pain, and that a shift toward M2a polarization (i.e., through EE or increased IL-11) may normalize excessive neuronal activity in nociceptive signaling pathways, and thus reduce migraine.

In summary, this study demonstrates that microglia and their polarization state are critical for SD induction. Specifically, M1 microglia produce ROS and pro-inflammatory cytokines, including TNF α which can alter neuronal excitability (Ajmone-Cat et al., 2013; Durafourt et al., 2012; Grinberg et al., 2012, 2013). M1 polarization may decrease inhibitory synaptic activity to promote initiation of SD (Kunkler et al., 2005; Pribiag and Stellwagen, 2013; Stellwagen et al., 2005). Furthermore, we demonstrate that a shift from M1 to M2a polarization is involved in EE-mediated increase of SD threshold. Thus, a better understanding of the mechanisms by which EE changes in microglia can mitigate SD will be important for the development of novel therapeutics for migraine.

Acknowledgment

Grant sponsor: National Institutes of Health Common Fund through the Office of Strategic Coordination/Office of the

Director; Grant number: 1-UH2 TR000918; and Grant sponsor: National Center for Advancing Translational Sciences of the National Institutes of Health; Grant number: UL1 TR000430; Grant sponsor: National Multiple Sclerosis Society; Grant number: IL-0009; Grant sponsor: National Institute of Neurological Disorders and Stroke; Grant number: NS-19108; Grant sponsor: National Institute of Child Health and Human Disorders; Grant number: 5 PO1 HD 09402; Grant sponsors: White Foundation and Cornell College Dimensions Fellowship provided by Dr. Elizabeth Becker (to J.K.).

The authors thank Y.Y. Grinberg for reading and commenting on the article. The authors thank Dr. C. Labno of the University of Chicago Light Microscopy Core for assistance with confocal imaging.

References

- Ajmone-Cat MA, Mancini M, De Simone R, Cilli P, Minghetti L. 2013. Microglial polarization and plasticity: evidence from organotypic hippocampal slice cultures. *Glia* 61:1698–1711.
- Brewer GJ, Torricelli JR, Evege EK, Price PJ. 1993. Optimized survival of hippocampal neurons in B27-supplemented Neurobasal, a new serum-free medium combination. *J Neurosci Res* 35:567–576.
- Bureš J, Burešová O, Krivánek J. 1974. The mechanism and applications of Leão's spreading depression of electroencephalographic activity. Prague: Academia.
- Caggiano AO, Kraig RP. 1998. Prostaglandin E₂ and 4-Aminopyridine prevent the lipopolysaccharide-induced outwardly rectifying potassium current and interleukin-1 β production in cultured rat microglia. *J Neurochem* 70:2357–2368.
- Chen Y, Stevens B, Chang J, Milbrandt J, Barres BA, Hell JW. 2008. NS21: Re-defined and modified supplement B27 for neuronal cultures. *J Neurosci Methods* 171:239–247.
- Chhor V, Le Charpentier T, Lebon S, Ore MV, Celador IL, Josserand J, Degos V, Jacotot E, Hagberg H, Savman K, Mallard C, Gressens P, Fleiss B. 2013. Characterization of phenotype markers and neuronotoxic potential of polarized primary microglia *in vitro*. *Brain Behav Immun* 32:70–85.
- Cook D, Sanchez-Carbente Mdel R, Lachance C, Radzioch D, Tremblay S, Khandjian EW, DesGroseillers L, Murai KK. 2011. Fragile X related protein 1 clusters with ribosomes and messenger RNAs at a subset of dendritic spines in the mouse hippocampus. *PLoS One* 6:e26120.
- Darabaneanu S, Overath CH, Rubin D, Luthje S, Sye W, Niederberger U, Gerber WD, Weisser B. 2011. Aerobic exercise as a therapy option for migraine: A pilot study. *Int J Sports Med* 32:455–460.
- Devinsky O, Vezzani A, Najjar S, De Lanerolle NC, Rogawski MA. 2013. Glia and epilepsy: Excitability and inflammation. *Trends in Neurosci* 37:174–184.
- Dreier JP, Major S, Pannek HW, Woitzik J, Scheel M, Wiesenthal D, Martus P, Winkler MKL, Hartings JA, Fabricius M, Speckmann EJ, Gorji A, COSBID study group. 2011. Spreading convulsions, spreading depolarizations and epileptogenesis in human cerebral cortex. *Brain* 135:259–275.
- Dringen R. 2005. Oxidative and antioxidative potential of brain microglial cells. *Antioxid Redox Signal* 7:1223–1233.
- Durafourt BA, Moore CS, Zammit DA, Johnson TA, Zaguia F, Guiot MC, Bar-Or A, Antel JP. 2012. Comparison of polarization properties of human adult microglia and blood-derived macrophages. *Glia* 60:717–727.
- Eder C, Schilling T, Heinemann U, Haas D, Hailer N, Nitsch R. 1999. Morphological, immunophenotypical and electrophysiological properties of resting microglia *in vitro*. *Eur J Neurosci* 11:4251–4261.

- Fares RP, Belmeguenai A, Sanchez PE, Kouchi HY, Bodennec J, Morales A, Georges B, Bonnet C, Bouvard S, Sloviter RS, Bezin L. 2013. Standardized environmental enrichment supports enhanced brain plasticity in healthy rats and prevents cognitive impairment in epileptic rats. *PLoS One* 8:e53888
- Fabel K, Wolf SA, Ehninger D, Babu H, Leal-Galicia P, Kempermann G. 2009. Additive effects of physical exercise and environmental enrichment on adult hippocampal neurogenesis in mice. *Front Neurosci* 3:50.
- Frei K, Bodmer S, Schwerdel C, Fontana A. 1986. Astrocyte-derived interleukin 3 as a growth factor for microglia cells and peritoneal macrophages. *J Immunol* 137:3521–3527.
- Fuente Mde L, Cruces J, Hernandez O, Ortega E. 2011. Strategies to improve the functions and redox state of the immune system in aged subjects. *Curr Pharm Des* 17:3966–3993.
- Ghezzi P, Bonetto V. 2003. Redox proteomics: Identification of oxidatively modified proteins. *Proteomics* 3:1145–1153.
- Gidday JM. 2006. Cerebral preconditioning and ischemic tolerance. *Nat Rev Neurosci* 7:437–448.
- Girard S, Brough D, Lopez-Castejon G, Giles J, Rothwell NJ, Allan SM. 2013. Microglia and macrophages differentially modulate cell death after brain injury caused by oxygen deprivation in organotypic brain slices. *Glia* 61:813–824.
- Grafstein B. 2011. Subverting the hegemony of the synapse: Complicity of neurons, astrocytes, and vasculature in spreading depression and pathology of the cerebral cortex. *Brain Res Rev* 66:123–132.
- Grinberg YY, Milton JG, Kraig RP. 2011. Spreading depression sends microglia on Lévy flights. *PLoS One* 6:e19294.
- Grinberg YY, van Drongelen W, Kraig RP. 2012. Insulin-like growth factor-1 lowers spreading depression susceptibility and reduces oxidative stress. *J Neurochem* 122:221–229.
- Grinberg YY, Dibbern ME, Levasseur VA, Kraig RP. 2013. Insulin-like growth factor-1 abrogates microglial oxidative stress and the TNF α responses to spreading depression. *J Neurochem* 126:662–672.
- Guedes RC, Monterio JS, Teodosio NR. 1996. Malnutrition and brain function: experimental studies using the phenomenon of cortical spreading depression. *Rev Bras Biol* 56:293–301.
- Herring A, Blome M, Ambree O, Sachser N, Paulus W, Keyvani K. 2010. Reduction of cerebral oxidative stress following environmental enrichment in mice with Alzheimer-like pathology. *Brain Pathol* 20:166–175.
- Hounsgaard J, Nicholson C. 1983. Potassium accumulation around individual Purkinje cells in cerebellar slices from the guinea-pig. *J Physiol* 340:359–388.
- Hulse RE, Swenson WG, Kunkler PE, White DM, Kraig RP. 2008. Monomeric IgG is neuroprotective via enhancing microglial recycling endocytosis and TNF- α . *J Neurosci* 25:3952–3961.
- Kariko K, Weissman D, Welsh FA. 2004. Inhibition of toll-like receptor and cytokine signaling – A unifying theme in ischemic tolerance. *J Cereb Blood Flow Metab* 24:1288–1304.
- Kigerl KA, Gensel JC, Ankeny DP, Alexander JK, Donnelly DJ, Popovich PG. 2009. Identification of two distinct macrophage subsets with divergent effects causing either neurotoxicity or regeneration in the injured mouse spinal cord. *J Neurosci* 29:13435–13444.
- Kobayashi K, Imagama S, Ohgomori T, Hirano K, Uchimura K, Sakamoto K, Hirakawa A, Takeuchi H, Suzumura A, Ishiguro N, Kadomatsu K. 2013. Minoxidil selectively inhibits M1 polarization of microglia. *Cell Death Dis* 4:e525.
- Kovacs R, Papageorgiou I, Heinemann U. 2011. Slice cultures as a model to study neurovascular coupling and blood brain barrier *in vitro*. *Cardiovasc Psychiatry Neurol* 2011:646958.
- Kraig RP, Dong LM, Thisted R, Jaeger CB. 1991. Spreading depression increases immunohistochemical staining of glial fibrillary acidic protein. *J Neurosci* 11:2187–2198.
- Kraig RP, Mitchell HM, Cristie-Pope B, Kunkler PE, White DM, Tang YP, Langan G. 2010. TNF α and microglial hermetic involvement in neurological health & migraine. *Dose Response* 8:389–413.
- Kreutz S, Koch M, Bottger C, Ghadban C, Korf HW, Dehghani F. 2009. 2-Arachidonoylglycerol elicits neuroprotective effects on excitotoxically lesioned dentate gyrus granule cells via abnormal-cannabidiol-sensitive receptors on microglial cells. *Glia* 57:286–294.
- Kruger H, Luhmann HJ, Heinemann U. 1996. Repetitive spreading depression causes selective suppression of GABAergic function. *Neuroreport* 10:2651–2656.
- Kudo C, Nozari A, Moskowitz MA, Ayata C. 2008. The impact of anesthetics and hyperoxia on cortical spreading depression. *Exp Neurol* 212:201–206.
- Kunkler PE, Hulse RE, Kraig RP. 2004. Multiplexed cytokine protein expression profiles from spreading depression in hippocampal organotypic cultures. *J Cereb Blood Flow Metab* 24:829–839.
- Kunkler PE, Hulse RE, Schmitt MW, Nicholson C, Kraig RP. 2005. Optical current source density analysis in hippocampal organotypic culture shows that spreading depression occurs with uniquely reversing currents. *J Neurosci* 25:3952–3961.
- Kunkler PE, Kraig RP. 1997. Reactive astrocytosis from excitotoxic injury in hippocampal organ culture parallels that seen *in vivo*. *J Cereb Blood Flow Metab* 17:26–43.
- Kunkler PE, Kraig RP. 1998. Calcium waves precede electrophysiological changes of spreading depression in hippocampal organ cultures. *J Neurosci* 18:3416–3425.
- Kunkler PE, Kraig RP. 2004. P/Q Ca²⁺ channel blockade stops spreading depression and related pyramidal neuron Ca²⁺ rise in hippocampal organ culture. *Hippocampus* 14:356–367.
- Lapilover EG, Lippmann K, Salar S, Maslarova A, Dreier JP, Heinemann U, Friedman A. 2012. Peri-infarct blood-brain barrier dysfunction facilitates induction of spreading depolarization associated with epileptiform discharges. *Neurobiol Dis* 48:495–506.
- Liao B, Zhao W, Beers DR, Henkel JS, Appel SH. 2012. Transformation from a neuroprotective to a neurotoxic microglial phenotype in a mouse model of ALS. *Exp Neurol* 237:147–152.
- Liu XF, Fawcett JR, Thorne RG, DeFor TA, Frey WH II. 2001. Intranasal administration of insulin-like growth factor-1 bypasses the blood-brain barrier and protects against focal cerebral ischemic damage. *J Neurol Sci* 187:91–97.
- Lochhead JJ, Thorne RG. 2012. Intranasal delivery of biologics to the central nervous system. *Adv Drug Deliv Rev* 64:614–628.
- Maiorino C, Khoroshi R, Ruffini F, Lobner M, Bergami A, Garzetti L, Martino G, Owen T, Furlan R. 2013. Lentiviral-mediated administration of IL-25 in the CNS induces alternative activation of microglia. *Gene Ther* 20:487–496.
- Mandavilli BS, Janes MS. 2010. Detection of intracellular glutathione using ThiolTracker violet stain and fluorescence microscopy. *Curr Protoc Cytom Chapter* 9:Unit 9.35.
- Marashi V, Barnekow A, Ossendorf E, Sachser N. 2003. Effects of different forms of environmental enrichment on behavioral, endocrinological, and immunological parameters in male mice. *Horm Behav* 43:281–292.
- Markovic DS, Glass R, Synowitz M, van Rooijen N, Kettenmann H. 2005. Microglia stimulate the invasiveness of glioma cells by increasing the activity of metalloprotease-2. *J Neuropathol Exp Neurol* 64:754–762.
- Martins-Ferreira H, Nedergaard M, Nicholson C. 2000. Perspectives on spreading depression. *Brain Res Rev* 32:215–234.
- Maheshwari A, Janssens K, Bogie J, Van Den Haute C, Struys T, Lambrechts I, Baekelandt V, Stinissen P, Hendriks JJ, Slaets H, Hellings N. 2013. Local overexpression of interleukin-11 in the central nervous system limits demyelination and enhances remyelination. *Mediators Inflamm* 2013:685317.

- Mitchell HM, White DM, Domowicz MS, Kraig RP. 2011. Cold preconditioning neuroprotection depends on TNF α and is enhanced by blockade of interleukin-11. *J Neurochem* 117:187–196.
- Mitchell HM, White DM, Kraig RP. 2010. Strategies for study of neuroprotection from cold-preconditioning. *J Vis Exp* 43:2192.
- Obiang P, Maubert E, Bardou I, Nicole O, Launay S, Bezin L, Vivien D, Agin V. 2011. Enriched housing reverses age-associated impairment of cognitive functions and tPA-dependent maturation of BDNF. *Neurobiol Learn Mem* 96:121–129.
- Olson AK, Eadie BD, Ernst C, Christie BR. 2006. Environmental enrichment and voluntary exercise massively increase neurogenesis in the adult hippocampus via dissociable pathways. *Hippocampus* 16:250–260.
- Pfaffl MW. 2001. A new mathematical model for relative quantification in real-time RT-PCR. *Nucleic Acids Res* 29:e45.
- Pietrobon D, Moskowitz MA. 2013. Pathophysiology of migraine. *Annu Rev Physiol* 75:365–391.
- Pomper JK, Haack S, Petzold GC, Buchheim K, Gabriel S, Hoffman U, Heinemann U. 2006. Repetitive spreading depression-like events result in cell damage in juvenile hippocampal slice cultures maintained in normoxia. *J Neurophysiol* 95:355–368.
- Pribiag H, Stellwagen D. 2013. TNF α downregulates inhibitory neurotransmission through protein phosphatase 1-dependent trafficking of GABA $_A$ receptors. *J Neurosci* 33:15879–15893.
- Pusic AD, Grinberg YY, Mitchell HM, Kraig RP. 2011. Modeling neural immune signaling of episodic and chronic migraine using spreading depression in vitro. *J Vis Exp* 52:2910.
- Pusic AD, Kraig RP. 2014. Youth and environmental enrichment generate serum exosomes containing miR-219 that promote CNS myelination. *Glia* 62:284–299.
- Pusic AD, Pusic KM, Kraig RP. 2014. IFN γ -stimulated dendritic cell exosomes as a potential therapeutic for remyelination. *J Neuroimmunol* 266:12–23.
- Pusic KM, Pusic AD, Kraig RP. 2013. Microglia are essential for spreading depression. *Soc Neurosci* 39:812.02.
- Radak Z, Chung HY, Goto S. 2008. Systemic adaptation to oxidative challenge induced by regular exercise. *Free Radic Biol Med* 44:153–159.
- Ransohoff RM, Perry VH. 2009. Microglial physiology: unique stimuli, specialized responses. *Annu Rev Immunol* 27:119–145.
- Rodriguez M, Sabate M, Rodriguez-Sabate C, Morales I. 2013. The role of non-synaptic extracellular glutamate. *Brain Res Bull* 93:17–26.
- Roundtree RB, Mandl SJ, Nachtwey JM, Dalpozzo K, Do L, Lombardo JR, Schoonmaker PL, Brinkmann K, Dirmeier U, Laus R, Delcayre A. 2011. Exosome targeting of tumor antigens expressed by cancer vaccines can improve antigen immunogenicity and therapeutic efficacy. *Cancer Res* 71:5235–5244.
- Sasaki S, Matsuura T, Takahashi R, Iwasa T, Watanabe H, Shirai K, Nakamoto H, Goto S, Akita S, Kobayashi Y. 2013. Effects of regular exercise on neutrophil functions, oxidative stress parameters and antibody responses against 4-hydroxy-2-nonenal adducts in middle aged humans. *Exerc Immunol Rev* 19:60–71.
- Schuchmann S, Meierkord H, Stenkamp K, Breustedt J, Windmuller O, Heinemann U, Buchheim K. 2002. Synaptic and nonsynaptic ictogenesis occurs at different temperatures in submerged and interface rat brain slices. *J Neurophysiol* 87:2929–2935.
- Shatillo A, Koroleva K, Giniatullina R, Naumenko N, Slastnikova AA, Aliev AA, Bart RR, Atalay M, Gu C, Khazipov B, Grohn O, Ginniatullin R. 2013. Cortical spreading depression induces oxidative stress in the trigeminal nociceptive system. *Neuroscience* 253:341–349.
- Sievers J, Schmidtmer J, Parwaresch R. 1994. Blood monocytes and spleen macrophages differentiate into microglia-like cells when cultured on astrocytes. *Ann Anat* 176:45–51.
- Snow RW, Taylor CP, Dudek FE. 1983. Electrophysiological and optical changes in slices of rat hippocampus during spreading depression. *J Neurophysiol* 50:561–572.
- Somjen GG. 2001. Mechanisms of spreading depression and hypoxic spreading depression-like depolarization. *Physiol Rev* 81:1065–1096.
- Stellwagen D, Beattie EC, Seo JY, Malenka RC. 2005. Differential regulation of AMPA receptor and GABA receptor trafficking by tumor necrosis factor- α . *J Neurosci* 25:3219–3228.
- Stenzel-Poore MP, Stevens SL, King JS, Simon RP. 2007. Preconditioning reprograms the response to ischemic injury and primes the emergence of unique endogenous neuroprotective phenotypes: a speculative synthesis. *Stroke* 38:680–685.
- Tetrault S, Chever O, Sik A, Amzica F. 2008. Opening of the blood-brain barrier during isoflurane anesthesia. *Eur J Neurosci* 28:1330–1341.
- Thorne RG, Pronk GJ, Padmanabhan V, Frey WH II. 2004. Delivery of insulin-like growth factor-1 to the rat brain and spinal cord along olfactory and trigeminal pathways following intranasal administration. *Neuroscience* 127:481–496.
- Trepicchio WL, Bozza M, Pedneault G, Dorner AJ. 1996. Recombinant human IL-11 attenuates the inflammatory response through down-regulation of proinflammatory cytokine release and nitric oxide production. *J Immunol* 157:3627–3634.
- Trepicchio WL, Dorner AJ. 1998. The therapeutic utility of interleukin-11 in the treatment of inflammatory disease. *Expert Opin Investig Drugs* 7:1501–1504.
- Tsuda M, Beggs S, Salter MW, Inoue K. 2013. Microglia and intractable chronic pain. *Glia* 61:55–61.
- van Praag H, Kempermann G, Gage FH. 2000. Neural consequences of environmental enrichment. *Nat Rev Neurosci* 1:191–198.
- van Rooijen N. 1989. The liposome-mediated macrophage ‘suicide’ technique. *J Immunol Methods* 124:1–6.
- Viggiano A, Viggiano E, Valentino I, Monda M, De Luca B. 2011. Cortical spreading depression affects reactive oxygen species production. *Brain Res* 1368:11–18.
- Vinet J, Weering HR, Heinrich A, Kalin RE, Wegner A, Brouwer N, Heppner FL, Rooijen Nv, Boddeke HW, Biber K. 2012. Neuroprotective function for ramified microglia in hippocampal excitotoxicity. *J Neuroinflammation* 9:27.
- Williamson LL, Chao A, Bilbo SD. 2012. Environmental enrichment alters glial antigen expression and neuroimmune function in the adult rat hippocampus. *Brain Behav Immun* 26:500–510.
- Zhang XC, Kainz V, Burstein R, Levy D. 2011. Tumor necrosis factor- α induces sensitization of meningeal nociceptors mediated via local COX and p38 MAP actions. *Pain* 152:140–149.
- Zhang Y, Taveggia C, Melendez-Vasquez C, Einheber S, Raine CS, Salzer JL, Brosnan CF, John GR. 2006. Interleukin-11 potentiates oligodendrocyte survival and maturation, and myelin formation. *J Neurosci* 26:12174–12185.